WSRC-STI-2007-00692
Keywords: Corrosion,
L-Basin

# FY2005 and FY2006 Corrosion Surveillance Results for L-Basin

Savannah River National Laboratory
Materials Science and Technology

Publication Date: September 2007

**Washington Savannah River Company**
**Savannah River Site**
**Aiken, SC 29808**

This document was prepared in connection with work done under Contract No. DE-AC09-96SR18500 with the U. S. Department of Energy

DISCLAIMER

**DOCUMENT: WSRC-STI-2007-00692**

**Title: FY2005-2006 Corrosion Surveillance Results for L-Basin (U)**

**MS&T APPROVALS**

_____ Date: _____
Philip R. Vormelker, Author
SRNL-Materials Application & Process Technology Group
MATERIALS SCIENCE AND TECHNOLOGY

_____ Date: _____
Cynthia N. Foreman, Author
SRNL-MC&JT Laboratory
MATERIALS SCIENCE AND TECHNOLOGY

_____ Date: _____
Dennis. W. Vinson, Technical Review
SRNL-Materials Application & Process Technology Group
MATERIALS SCIENCE AND TECHNOLOGY

_____ Date: _____
Robert L. Sindelar, Manager
SRNL-Materials Application & Process Technology Group
MATERIALS SCIENCE AND TECHNOLOGY

_____ Date: _____
Natraj C. Iyer, Director
SRNL-MATERIALS SCIENCE AND TECHNOLOGY

**DOCUMENT: WSRC-STI-2007-00692**

**Title: FY2005 and FY2006 Corrosion Surveillance Results For L-Basin (U)**

**CUSTOMER APPROVALS**

_____

R. W. Deible, Engineer Date: _____
SFP Operations Engineering
OBU-SPENT FUEL PROJECT

## TABLE OF CONTENTS



## LIST OF ABBREVIATIONS

| | |
|---|---|
| CA | Contaminated Area |
| DOE | Department of Energy |
| DRR | Domestic Research Reactor |
| FRR | Foreign Research Reactor |
| HTS | Horizontal Tube Storage |
| MB | Machine Basin |
| MS&T | Materials Science and Technology |
| MTS | Materials Technology Section |
| PI | Principal Investigator |
| PPE | Personal Protective Equipment |
| PTFE | Polytetrafluoroethylene |
| RBOF | Receiving Basin for Offsite Fuel |
| SNF | Spent Nuclear Fuel |
| SRS | Savannah River Site |
| SRNL | Savannah River National Laboratory |
| SS | Stainless Steel |
| TB | Transfer Bay |
| VTS | Vertical Tube Storage |

## 1.0 SUMMARY

This report documents the results of the L-Basin Corrosion Surveillance Program for the fiscal years 2005 and 2006. The water quality and basin conditions for the coupon immersion period are compared to the corrosion evaluation results from detailed metallurgical analysis of the coupons.

Test coupons were removed from the basin on two occasions, March 29, 2005 and May 23, 2006, examined and photographed. Selected coupons were metallurgically characterized to evaluate the extent of general corrosion and pitting. Crystallographic and energy dispersive spectroscopy analysis were performed on a typical specimen, as-removed from the basin, to characterize the surface debris. Marked changes were noted in both the 2005 and 2006 specimens compared to previous years' corrosion results. A new pitting incidence has occurred on the faces of the aluminum coupons compared to localized pitting at crevice regions only on specimens withdrawn in 2003 and 2004. The pitting incidence is attributed to sand filter fines that entered the basin on July 27, 2004 from an inadvertent backflush of the new sand filter.

Pitting rate results show a trend of slowing down over time which is consistent with aluminum pit kinetics. Average pit growth rates were equal to or lower in all 2006 aluminum coupons than those removed in 2005. A trend line shows that pitting corrosion rates on Al1100, 6061, and 6063 coupons are slowing down since pit depth measurements were initiated in 2003.

No impact to stored spent fuel is expected from the debris. The storage configuration of the majority of L-Basin spent fuel, in bundles, should provide a measure of isolation from debris settling in the basin.

## 2.0 INTRODUCTION

Spent nuclear fuels from DOE-owned fuel used in foreign and domestic research and test reactors are currently being stored in the L-Basin. The corrosion surveillance program was initiated in 1992 with various coupon types immersed in SRS reactor basins. The present corrosion surveillance in L-Basin follows a corrosion surveillance plan [1]. The coupons removed for this report are from Junior Ray Guns which contain 36 coupons hanging in either vertical tube storage for the 2005 coupons or horizontal tube storage in L-Basin for the 2006 coupons. The 2005 coupons were withdrawn March 29, 2005 following immersion in L-Basin for 5 years 10 ½ months. The FY2006 coupons were withdrawn in May 23, 2006 following immersion in L-Basin for 7 years 20 days after initial placement in the Basin on May 15, 1999. The 2005 coupon removal included the first set of Junior Ray Gun coupons removed from L-Basin for corrosion evaluation. Prior to 2005, all extracted coupon sets were comprised of larger assemblies holding 70 coupons. These larger coupon assemblies, called Ray Guns, have been essentially used up while performing corrosion evaluations, with one assembly remaining for analysis at L-Basin closing.

## 3.0 CORROSION EVALUATION

### 3.1 Water Quality during Coupon Immersion

Only minor changes in water quality occurred due to multiple deionizer shutdowns throughout the immersion period of the surveillance coupons. Increases in conductivity, pH, and Cs-137 occurred when the deionizer was turned off (Figure A.1). The greatest changes happened during two periods; May 7 to July 28, 2004 (Cs-137 activity from 50 to 300 dpm/ml, conductivity

from 0.5 to 3 µS/cm, and pH from 6 to 7) and November 25, 2004 to March 20, 2005 (Cs-137 activity from 50 to 250 dpm/ml, conductivity from 1 to 5 µS/cm, and pH from 6.5 to 7). The basin water quality parameters remained within allowable limits (Table 1) at both of these times. During these same time periods, no changes in impurity levels (Cl, Al, Fe, and Hg) occurred as seen in Figure A.2. The data demonstrate that the basin water chemistry was not significantly altered by having the deionizers offline for up to 116 days.

**Table 1** L-Basin Water Quality Operating Limits

| Water Quality Parameters | Operating Limit | Monitoring Frequency |
|---|---|---|
| pH | 5.5 to 8.5 | Weekly |
| Conductivity | 10 µS/cm | Weekly |
| Activity | Cs-137: 500 dpm/ml<br>Alpha: 3 dpm/ml<br>Tritium: 0.4 µCi/ml<br>($8.88 \times 10^5$ dpm/ml) | Weekly<br>Monthly<br>Biannual |
| Cu Concentration | 0.1 ppm | Biannual |
| Hg Concentration | 0.014 ppm | Biannual |
| Cl Concentration | 0.1 ppm | Biannual |
| Fe | 1.0 ppm | Biannual |
| Al | 1.0 ppm | Biannual |
| Temperature | 40°C | Weekly |

The new sand filter was started on approximately July 27, 2004. After startup, sand filter fines populated the basin water and clouded the basin so that the bottom was barely visible. The fines from the sand filter later settled on all horizontal surfaces in the basin including the upper surfaces of the horizontally mounted surveillance coupons. Cs-137 levels dropped considerably after that day due to deionizer start-up on July 27th.

Water quality improved over the additional year of immersion for the 2006 coupons due to continuous deionizer operation as shown in Figure B.2. Conductivity and Cs-137 values leveled off at approximately 1.3 µS/cm and 40 dpm/ml, respectively while pH levels remained below 7, except for three excursions during October and November 2005. All impurity levels remained below operational limits as shown in Figure B.3.

### 3.2 Optical Evaluation of Corrosion Coupons from 2005 and 2006

As-received coupons are shown in Figure A.3 and Figure A.4 (2005) and Figure B.1 (2006). The coupon sets contain individual, crevice and galvanic coupons (1100, 6061, and 6063) mated with 304 SS. All coupons are 1.25 inches in diameter. All coupons were photographed. The oxide films, grown on the coupons during immersion, were removed with a 16M nitric acid solution (10 minutes minimum). Stirred immersions in an ultrasonic bath were performed with weights measured before and after each cleaning step to ensure oxide removal and not the removal of metal per ASTM Standard G-1 [2].

The set of 2005 galvanic coupons is shown in Figure A.3. Figure A.4 is a close-up that reveals the position of the Teflon PTFE (Polytetrafluoroethylene) washers (spacers) and the upward facing surface of a few coupons. The Face-Up side pointed up towards the water surface while hanging in L-Basin. A surface coating (yellow color) appears on the Face-Up side of most coupons. The colored surface is also visible in most of the as-received photos of the 30 aluminum coupons in the junior ray gun sets removed in 2005 (Figure A.5 through Figure A.20) and 2006 (Figure B.4 through Figure B.19). Distinguishing between the Face-Up versus the

Face-Down position of the coupon face was made to investigate the effects of orientation that may have occurred with settlement of debris.

Before and after cleaning photos of single coupons are shown in Figure A.5 through Figure A.20 for the 2005 coupon set and Figure B.4 through Figure B.19 for the 2006 coupons. For the 2005 and the 2006 coupons sets, the Face-Up side of each single coupon reveals the yellow-tan color on the surface. Pits are visible in the as-received surface of the Al 1100 #54 coupon (Figure A.7) and confirmed in the cleaned coupon.

Galvanic Coupon Specimen Sets: Galvanic coupon surfaces (mated with 304 stainless steel) are shown in Figure A.12 through Figure A.14 (2005) and Figure B.16 through Figure B.19 (2006). For the non-mating surface side, four out of the six aluminum coupons were facing up in the 2005 galvanic coupon set and coloring was not visible on these surfaces. In the 2006 galvanic coupon set, all non-mating surfaces of the aluminum coupons faced down. Large pits are visible below the Teflon washer area on an Al 6061 coupon (2006) on the side opposite to that mated to 304 stainless steel (Figure B.18).

Crevice Coupon Specimen Sets: Crevice coupon surfaces (two of the same alloy mated together) are shown in Figure A.15 through Figure A.20 (2005) and Figure B.10 through Figure B.15 (2006). All of the crevice coupon non-mating surfaces that faced up reveal the yellow-tan coloring on the surface. In Figure A.20, surface pitting is visible before and after cleaning on the Al 6063 #59 coupon.

Single Coupons: Examples of the 2005 coupons are shown in Figure A.21 through Figure A.23. The Al 1100 #055 coupon (Figure A.21) shows a few individual pits on the surface facing up in the basin. Figure A.22 shows 2-3 pits that formed below the PTFE washer on the Face-Up side of the coupon. Figure A.23 shows numerous pits on the Face-Up side of the Al 6063 #053 coupon. The higher number of pits shown on the 6063 coupon compared with the 1100 and 6061 coupons is attributed to end grain attack of the 6063 alloy.

### 3.3 Metallurgical Evaluation of Corrosion Coupons

Pit depth measurements were performed on all coupons using a measuring microscope with averages based on the 10 deepest pits per ASTM G46. Pit depth values for single coupons are graphed in Figure A.24 (2005). Pit depth averages and maximums for the 2005 Face-Up coupons (Al 1100 and Al 6061) are greater than or equal to the values (≤ 0.7 mil difference) for the Face-down coupons except for the low average pit depth for the Face-Up side of the Al 1100 #052 coupon. However, the same trend was not observed in the single 6063 coupons where the Face-Down side of the 2005 coupons exhibited higher pit depth averages than the Face-Up side (≤ 1 mil differences). In the 2006 single coupon set, pit depth averages and maximums for the Face-Up surfaces (Al 1100 and Al 6061) exhibited greater than or equal to the values for the Face-down surfaces (Figure B.24). All 6063 coupons revealed pit depth averages and maximums that were greater in the Face-Up surface versus the Face-down surface except for the #132 coupon which displayed higher average pit depths on the Face-down surface. However, the maximum pit depths were higher on the Face-Up surface.

Literature reports of effects of debris on aluminum [3] have indicated increased corrosion rates due to foreign particle deposition on the surface of water immersed aluminum coupons. The particles act as cathodes on the surface and the surrounding metal (anode) corrodes. This type of attack was observed in the L-Basin coupons. Energy dispersive spectroscopic (EDS) analysis was performed on selected 2006 corrosion coupons prior to cleaning to confirm the existence of foreign particles. EDS confirmed that sand particles containing Si, Ti, and Fe from

the sand filter release were present on a Al 1100 coupon surfaces as shown in Figure B.20. White areas on some coupons (Al1100 #039 and Al6061 #109) were analyzed by X-Ray diffraction (XRD) and contain elemental aluminum, Bayerite ($Al(OH)_3$), Quartz ($SiO_2$), and Moscovite ($H_2KAl_3(Si0_4)_3$) on both sides of the coupons. In addition, XRD analysis was performed on surface deposits from a sand filter media trap which contained Quartz ($SiO_2$), Hematite ($Fe_2O_3$), Fluorapatite ($Ca_5(PO_4)_3F$), Rutile ($TiO_2$), and Hematite ($Fe_2O_3$) [4] which were found in the sand deposits on the Al 1100 coupon.

Locations of the analyzed pits (e.g. beneath washer vs. on face) was not distinguished in this analysis. Average pit depths for all 2005 Al 1100 single coupons were ≤ 2 mils (Figure A.24). The average pit depths for the 2006 Al 1100 single coupons was ≤ 1.85 mils (Figure B.24). Average pit depths measured on the 2004 Al 1100 surveillance coupons were skewed due to one coupon with two pits measuring 3.1 mils and 14.3 mils and the other coupon with an average of 1.5 mils and a maximum of 2.2 mils. The average pit depth for the lone Al 1100 coupon from 2003 measured approximately 8 mils. The averages for the four 2005 coupons are slightly higher than the average for the 2004 single coupon even though the immersion time for the 2004 coupons was approximately 8 years versus 6 years for the 2005 coupons. This data is displayed in Figure B.21 showing that pit growth rate to be decreasing with time.

Pit depth averages for the 2005 Al 6061 single coupons were ≤ 2.0 mils, very similar to averages for the Al 1100 coupons (Figure A.24). The pit data from the two measured 2004 Al 6061 coupons revealed an average of ≤ 1.6 mils for one coupon while the other was measured with no pits ≥ 1 mil depth. The 2006 pit data from Al 6061 coupons (Figure B.24) also average 1.6 mils. These depths are very similar despite the two year difference in immersion time between the 2004 and 2005 coupons and one year difference between the 2004 and 2006 coupon immersion times. Average and maximum Al 6061 pit data is shown in Figure B.22 which also shows pit growth rate to be decreasing with time.

The average pit depth for the 2005 Al 6063 coupons ranged from 2.6-3.7 mils (A.24). These depth averages are higher than the Al 6063 coupon averages of 1.6 mils and 1.3 mils for single 2004 and 2003 Al 6063 coupons, respectively. In 2006, the Al 6063 coupons average pit depth was ≤ 3.6 mils (B.24). The Al 6063 pit depths (average and maximum) are graphed in Figure B.23 which also displays a decrease in rates as observed for Al 1100 and Al 6061.

Galvanic coupons for 2005 (Figure A.26) displayed average pit depths up to 15 mils on the mating side with 304 stainless steel in with a maximum depth less than 27 mils while pit depths in the 2006 galvanic coupons were also up to 15 mils on the mating side with maximum depths ≤ 20 mils (Figure B.26). The 2005 average pit depths on the open side of the coupons was less than or equal to 12 mils in depth with a maximum of 26 mils and 13 mils and 20 mils respectively for the 2006 coupons. In 2004, the averages were less than 6 mils on the open side of the coupon. However, the original data on the mating side of the Al 6063 coupon from 2004 revealed a maximum pit depth of 14 mils. The 2005 galvanic couples are the same diameter (both 1.25 inches outside diameter) while previous galvanic coupons were 2.75 inch diameter 304 stainless steel coupon mated to a 1.25 inch diameter aluminum alloy.

The most recent full Ray Gun set of coupons was analyzed in 2004. This set also contained additional galvanic coupons which mated a large 2.75 inch diameter 304 stainless steel or aluminum alloy with a different 1.25 inch diameter aluminum alloy. The averages for these coupons were less than or equal to 2.2 mils with very little differences in pit depths between the large coupon and the smaller one since despite the area difference between the two alloys. Maximum pit depths were less than or equal to 2 mils with three maximum pit depths up to 7 mils. This type of coupon couple was not repeated in the Junior Ray Gun which contained

matching aluminum alloy pairs, both 1.25 inch diameters. These matching pairs are called crevice coupons in because there are no electrochemical differences between the same alloy mating coupons. Electrochemical differences result in higher pit depths as shown by the results from the galvanic coupons mated with stainless steel. The 2005 pit depth averages for all but one set of crevice coupons are less than or equal to 2.5 mils (Figure A.26). However, there was one average pit depth that was closer to 4 mils (Al 6063 059). The 2.5 mil average depth is equivalent to the different sized coupon pairs (different alloys) from Figure 13 in Reference [5]. The 2006 pit depth averages for the crevice coupons (Figure B.25) are ≤ 3.6 mils in the face-up orientation and ≤ 4.7 mils in the face-down orientation.

Pit growth rates of the three coupon types in Figure A.27 are generated from pit depths by dividing the average pit depth (both sides) by the immersion time (i.e. 70.5 months/5.9 years for the 2005 coupons). The growth rate for non-304 mated coupon pairs is approximately 0.5 mil/yr or less as calculated for the approximate 5.9 year immersion period. A pit growth rate of ≤ 0.3 mil/yr was reported in 2004 for non-304 mated coupon pairs. A pit growth rate of ≤ 1 mil/yr was measured on the single aluminum coupons for 2003 while growth rates for 2005 and 2006 (Figure B.27) single aluminum coupons were ≤ 0.55 mil/yr.

To determine the pit density (No. pits/$mm^2$), the number of pits (≥ 0.001 inch in depth) was counted within three 0.03 x 0.03 $in^2$ areas (0.5809 $mm^2$) on each coupon. Pit density was not reported when the total number of pits was less than 50 in three square areas. Single coupon pit densities (both sides) are shown in Figure A.28 for 2005. For all but one coupon, the average pit density is ≤ 62 pits/$mm^2$ while the highest average pit density was 110 pits/$mm^2$ for a 6061 coupon surface in the Face-Up orientation. In the six coupons where pit densities were measured on both surfaces, the maximum density was higher in the Face-Up orientation in five out of the six coupons. However the average density was higher in the Face-Down orientation in four out of the six coupons. In 2006, pit densities for single coupons average ≤ 65 pits/$mm^2$. However, there was not a clear trend towards higher densities in the Face-Up orientation (Figure B.28).

Pit densities for 2005 galvanic and crevice coupon pairs are shown in Figure A.29. Mating surfaces show higher pit densities in half of the galvanic coupon pairs while the remaining half reveals a significantly lower number of pits. In most crevice coupon pairs, the coupon surface in the face down position reveals higher pit densities for most of the pairs. However, one coupon surface in the face-up orientation (6061 #067 w/#) has the highest average and maximum pit densities. For 2006 galvanic and crevice coupon pairs, pit densities are shown in Figure B.29. However, the lack of pit density data makes it difficult to establish a trend towards higher pit densities in the Face-up orientation.

Original data for 2005 and 2006 corrosion surveillances are contained in logbooks in References [6] and [7].

## 3.0 CONCLUSIONS

The following conclusions are drawn from the analysis of the corrosion surveillance coupons immersed in L-Basin:

- Sand was identified on both top and bottom surfaces of aluminum coupons. However no effects on pit depths were determined except that a few pits were visible on surface oxides prior to acid cleaning..

- Pit growth rates have decreased for the single aluminum coupons. Specifically, in 2003, pit growth average rates of ≤ 1 mil/yr (mpy) were observed while rates for 2005 and 2006 were ≤ 0.49 mpy and ≤ 0.44 mpy, respectively.

## 4.0 REFERENCES

1. P. R. Vormelker, “L-Basin Corrosion Surveillance Program Plan,” WSRC-TR-2006-00008, April 2006.
2. ASTM Standard G-1, “Standard Practice for Preparing, Cleaning, and Evaluating Corrosion Test Specimens,” October 1, 2003.
3. Roberto Haddad. Presentation, IAEA’s Consultancy Meeting "Guidelines for Management of Water Quality in Research Reactors”, Vienna, Austria, 15 – 17 May 2006.
4. A. D. Reedy, Analysis of Sand Filter Trap Media, e-mail message to P. R. Vormelker (7/16/2007).
5. P. R. Vormelker, A. J. Duncan and T. H. Murphy, “FY2004 Corrosion Surveillance Results for L-Basin (U), WSRC-TR-2005-00067, September 2005.
6. Logbook, L-Basin Coupon Corrosion Surveillance 2005, WSRC-NB.2005-00014, p 1-139.
7. Logbook, L-Basin Coupon Corrosion Surveillance 2006, WSRC-NB.2006-00129, p 1-70.

# Appendix A

## Coupon Photos and Data Graphs from FY2005 Corrosion Surveillance

### List of Figures

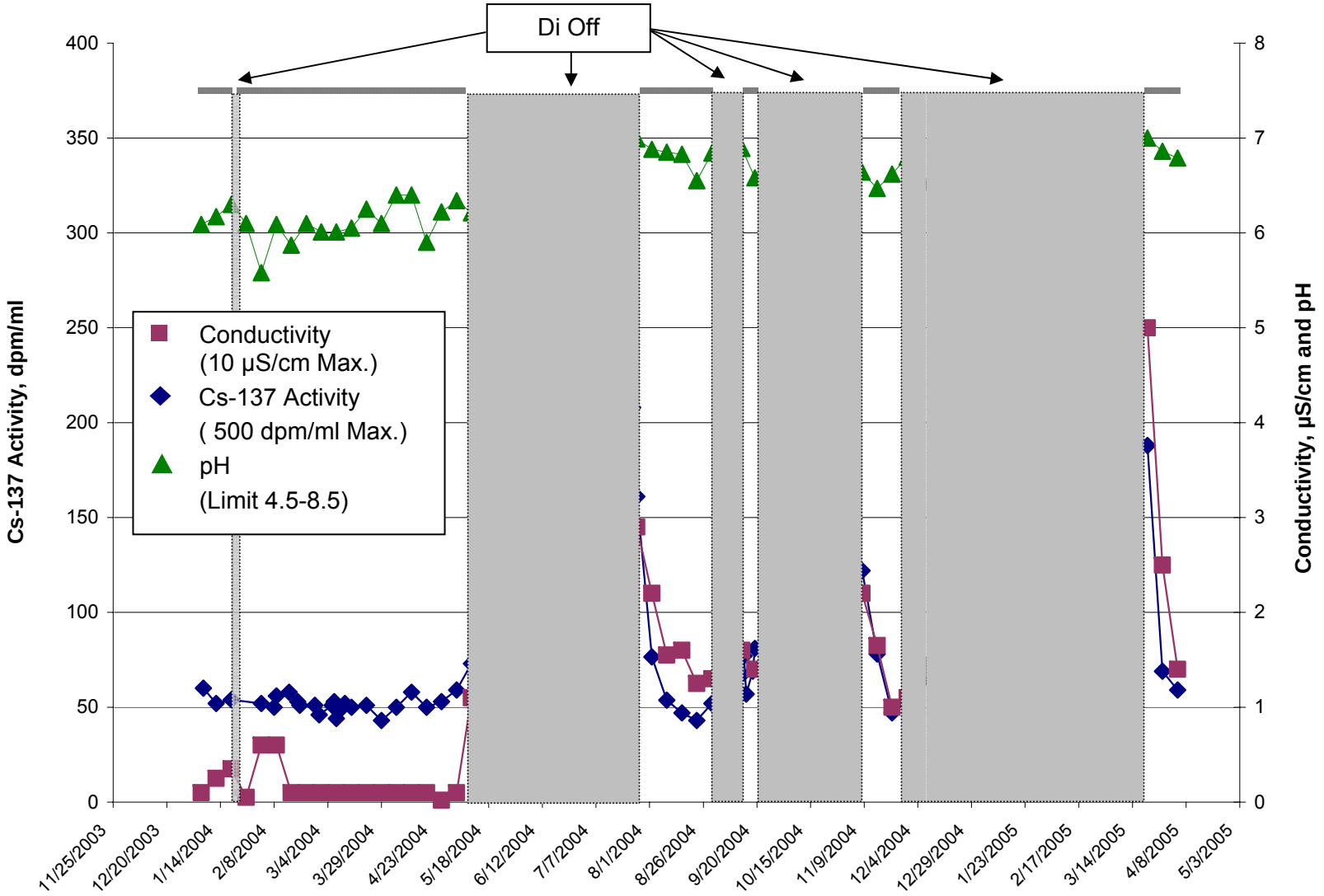


Figure A.1 Time dependent conductivity, pH and Cs-137 in L-Basin during the period January 2004 to May 2005.

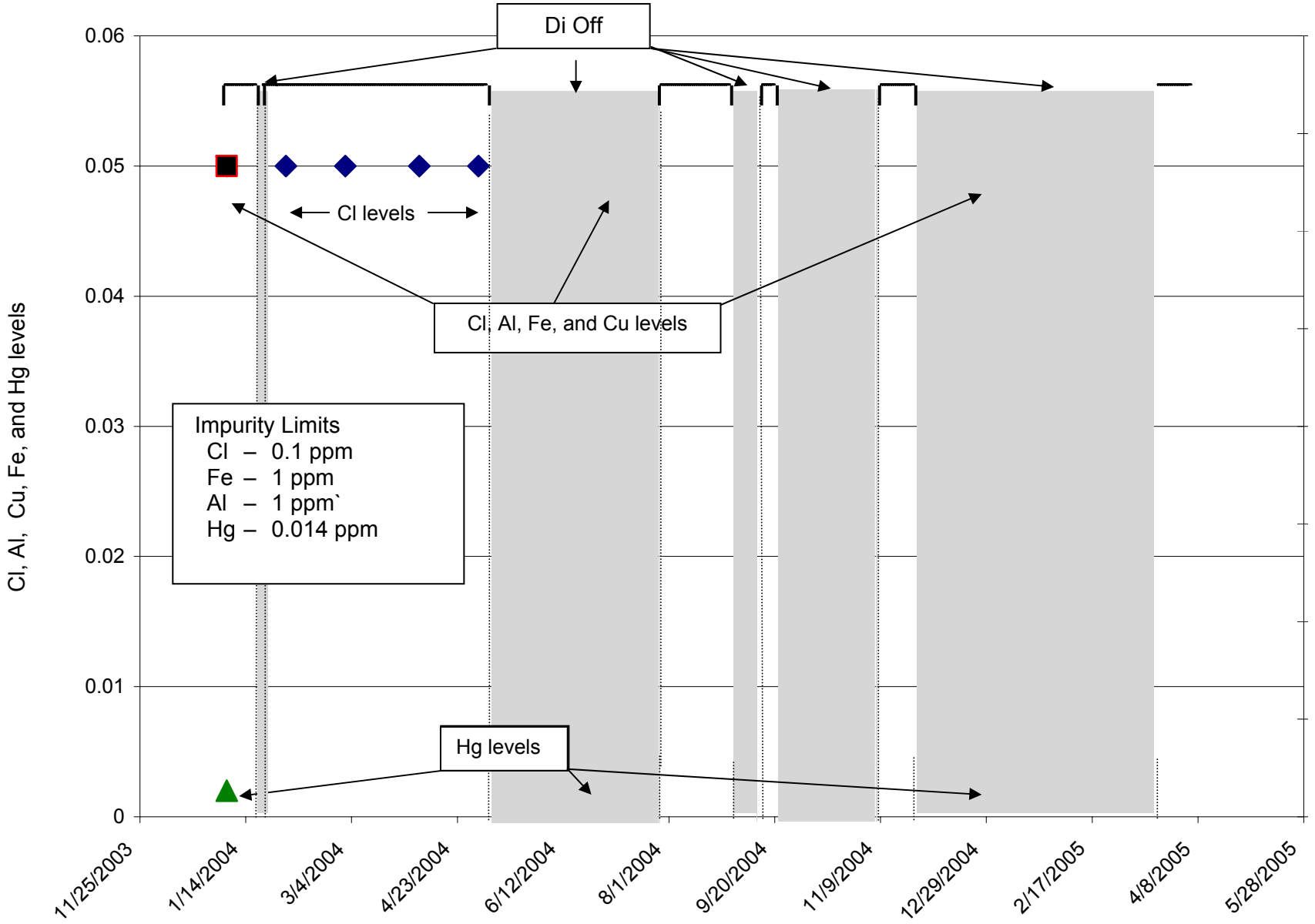


Figure A.2 Time dependent impurity levels in L-Basin during the period January 2004 to May 2005. Each data point is below detectible limits. No changes occurred in these levels over the time period.

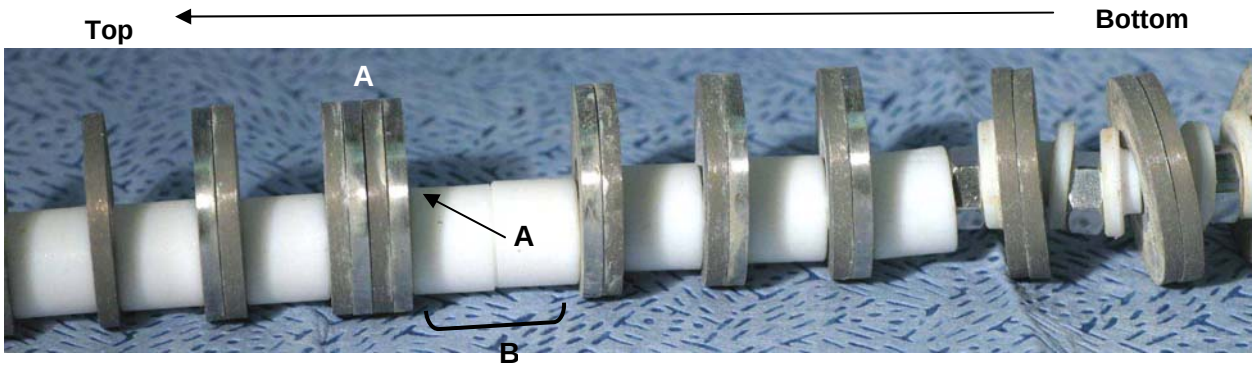


Figure A.3 Close-up of double set of galvanic coupons at position A with two PTFE spacers (B) on the right.

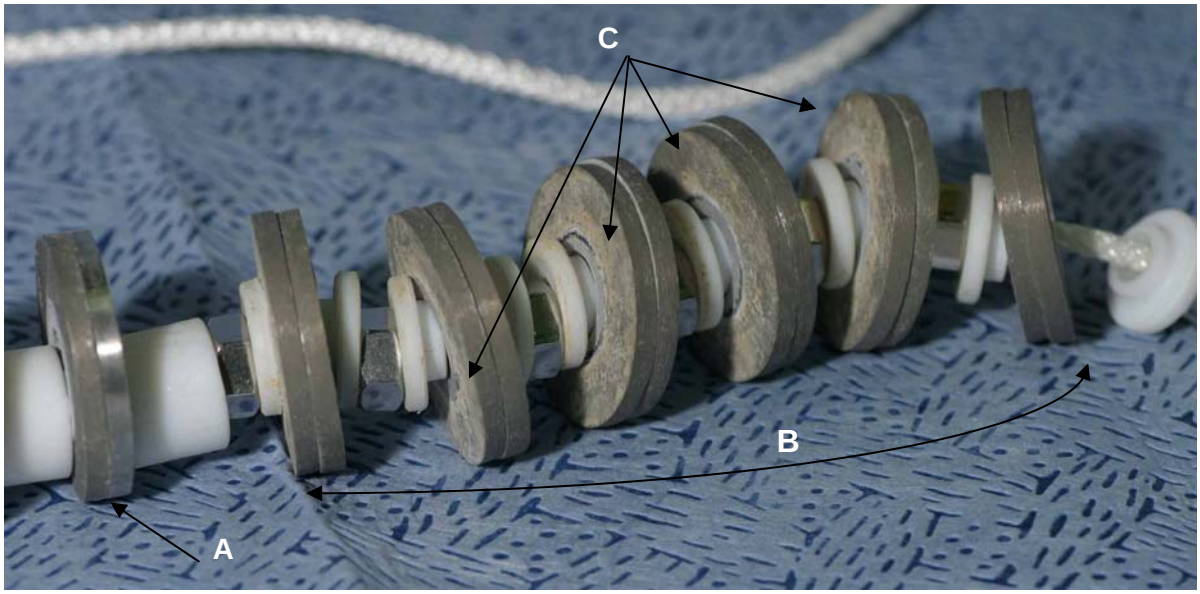


Figure A.4 Close-up view of the surveillance coupons showing coupled coupons with Teflon insulating washers (spacers) that were removed from the rod used during immersion and placed on a string for transport to SRNL. A galvanic couple (stainless/aluminum) is visible at A and the remainder of the coupled coupons in the photograph at B are crevice type. Yellow/tan coloring is visible on the face-up surface of the coupons (C).

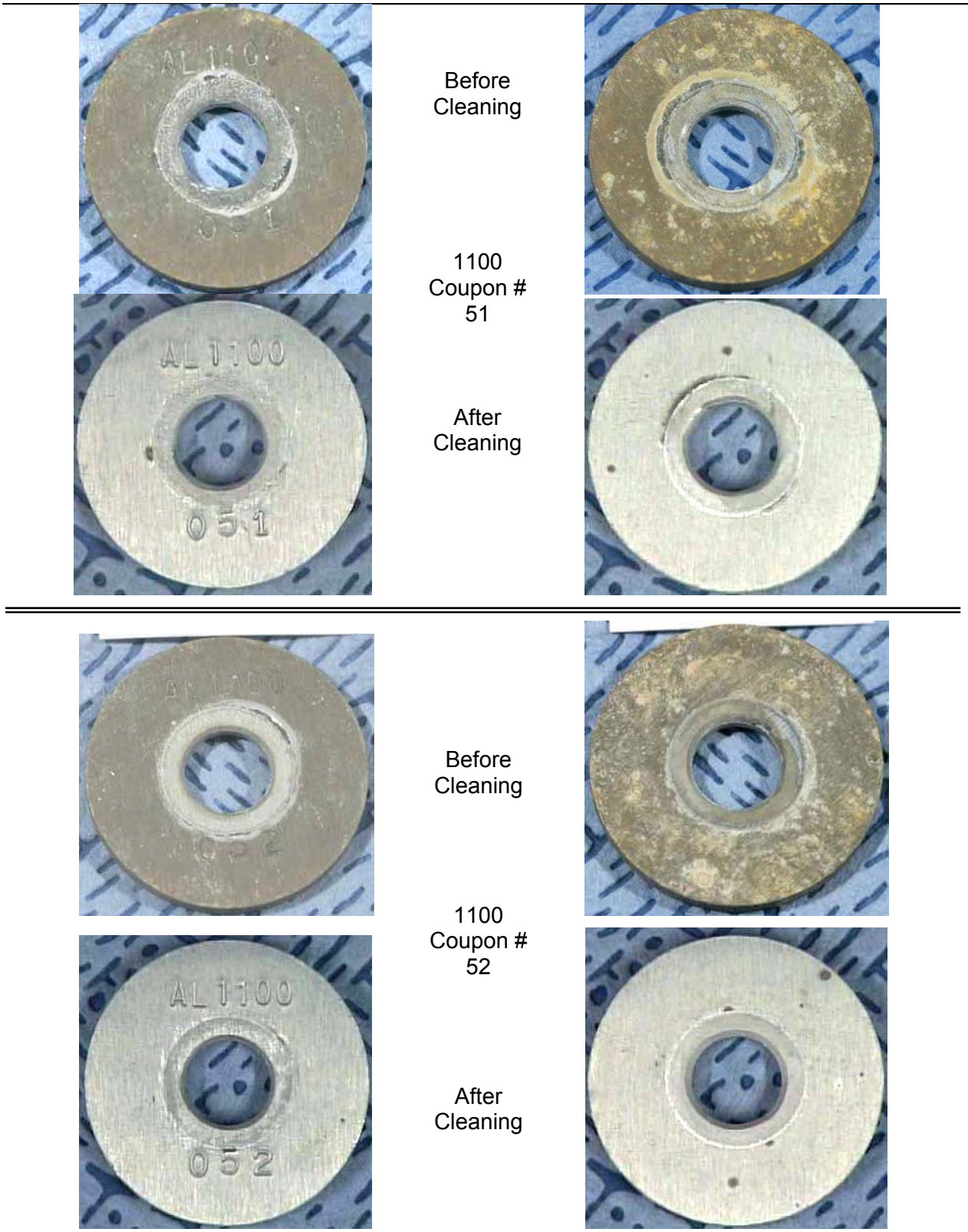


Figure A.5 Photos taken before and after cleaning of single 1100 coupons, #'s 51 and 52. The yellow/tan coloring is visible on the Face-Up side (w/o #) of the two 1100 coupons.

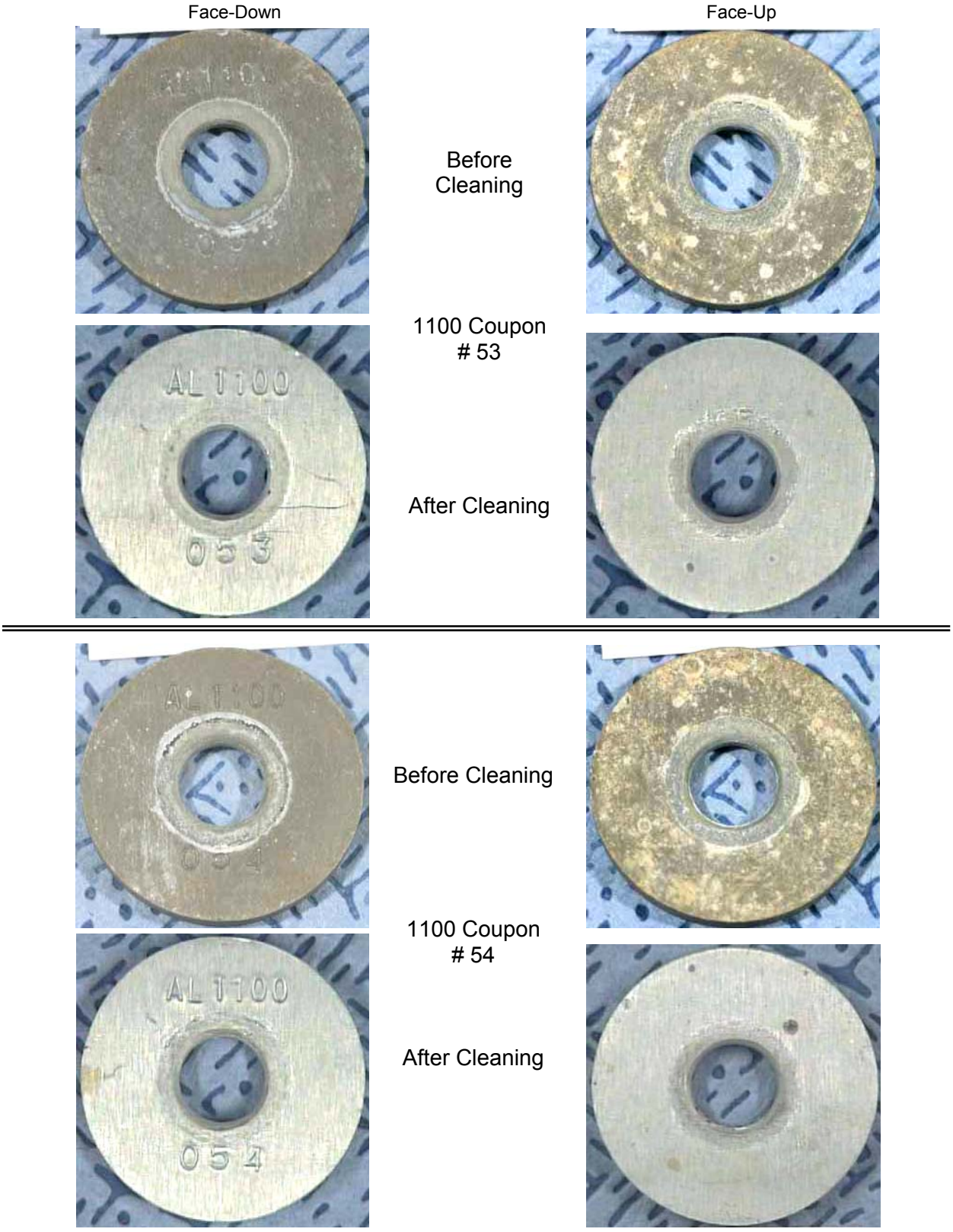


Figure A.6 Photos taken before and after cleaning of single 1100 coupons, #'s 53 and 54.

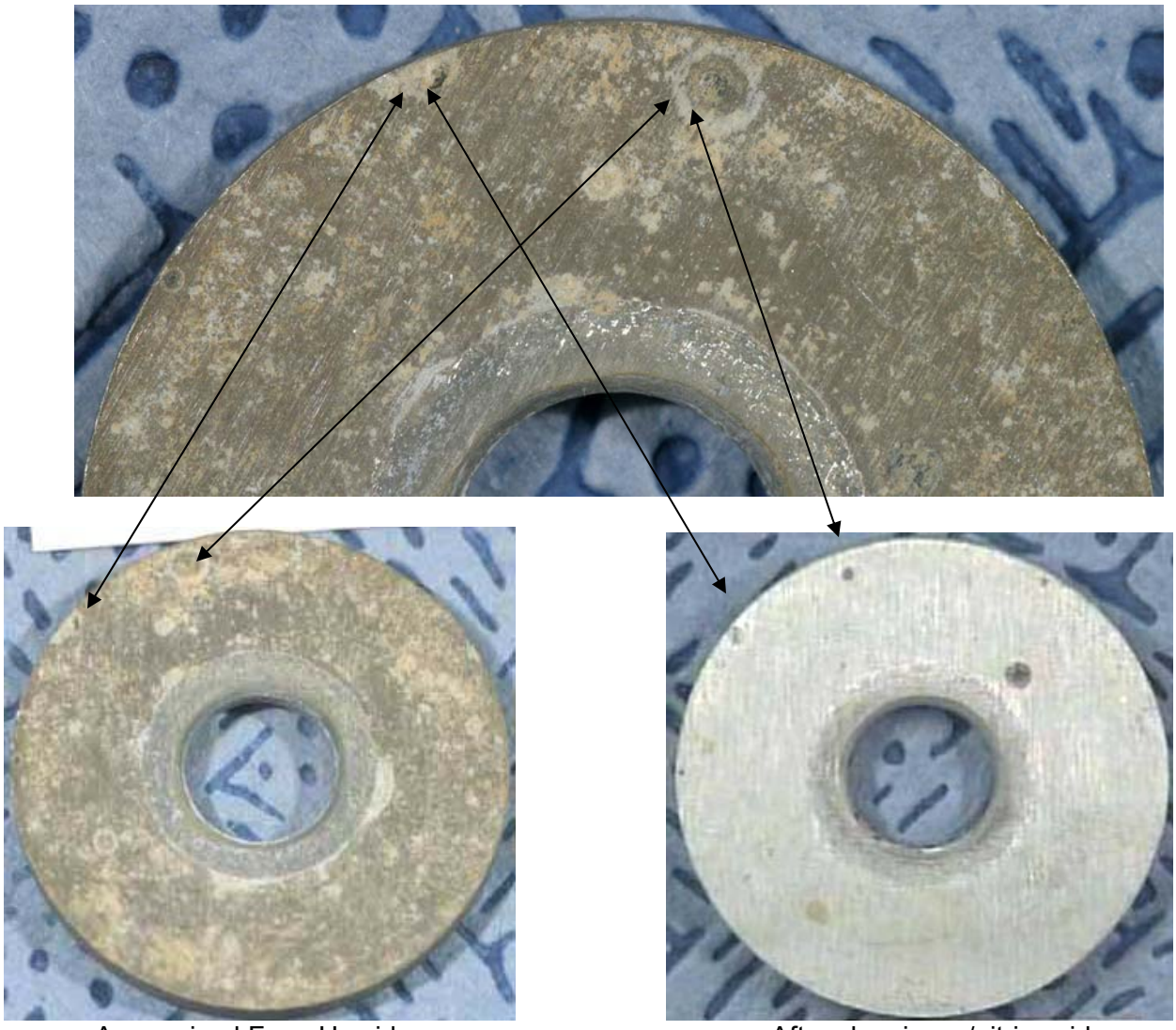

As-received Face-Up side

After cleaning w/nitric acid

Figure A.7 Comparison of individual coupon 1100 # 54 with a few deep pits shown after cleaning with the same pits visible in as-received coupon.

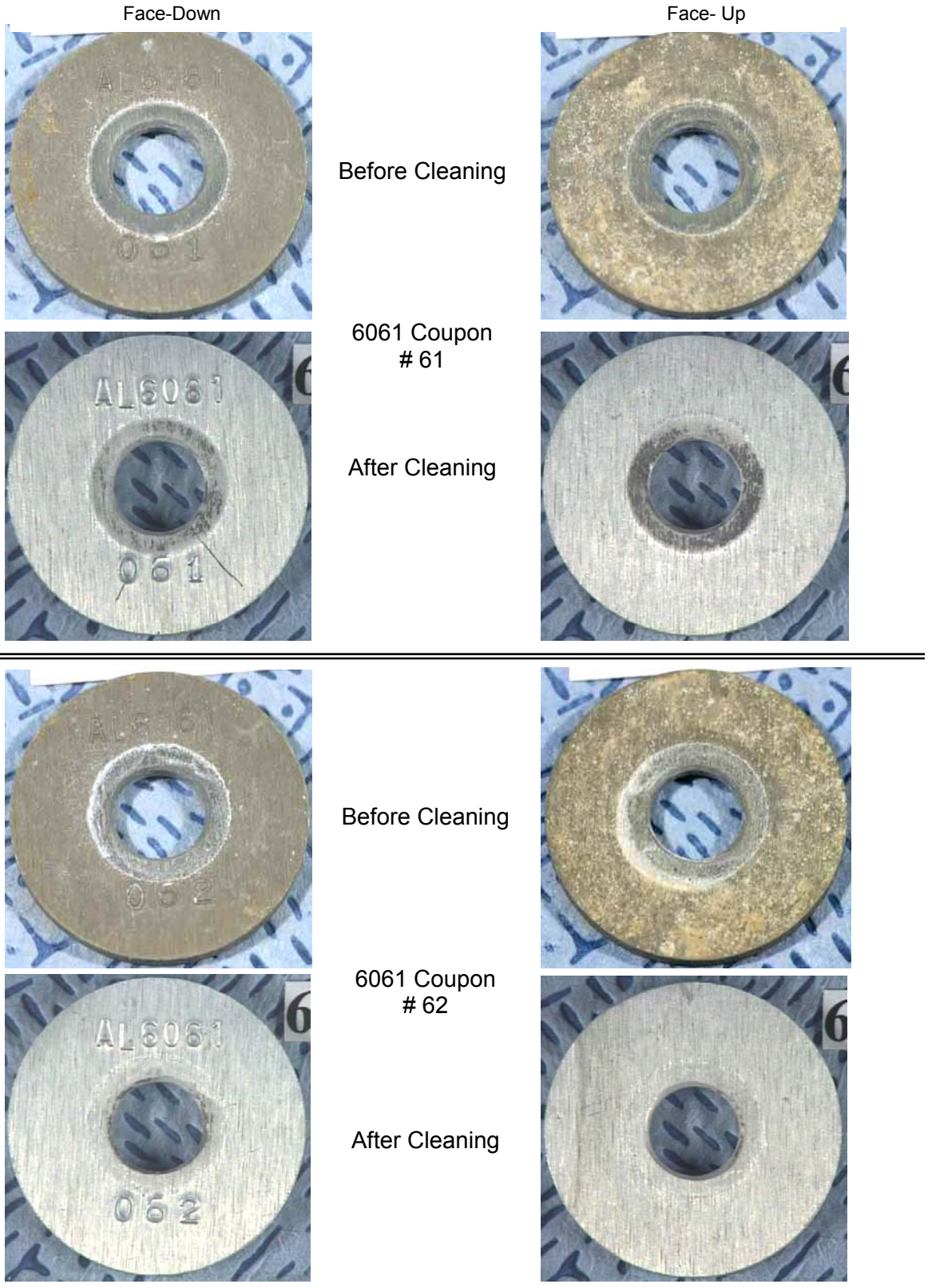


Figure A.8 Photos taken before and after cleaning of single 6061 coupons, #'s 61 and 62.

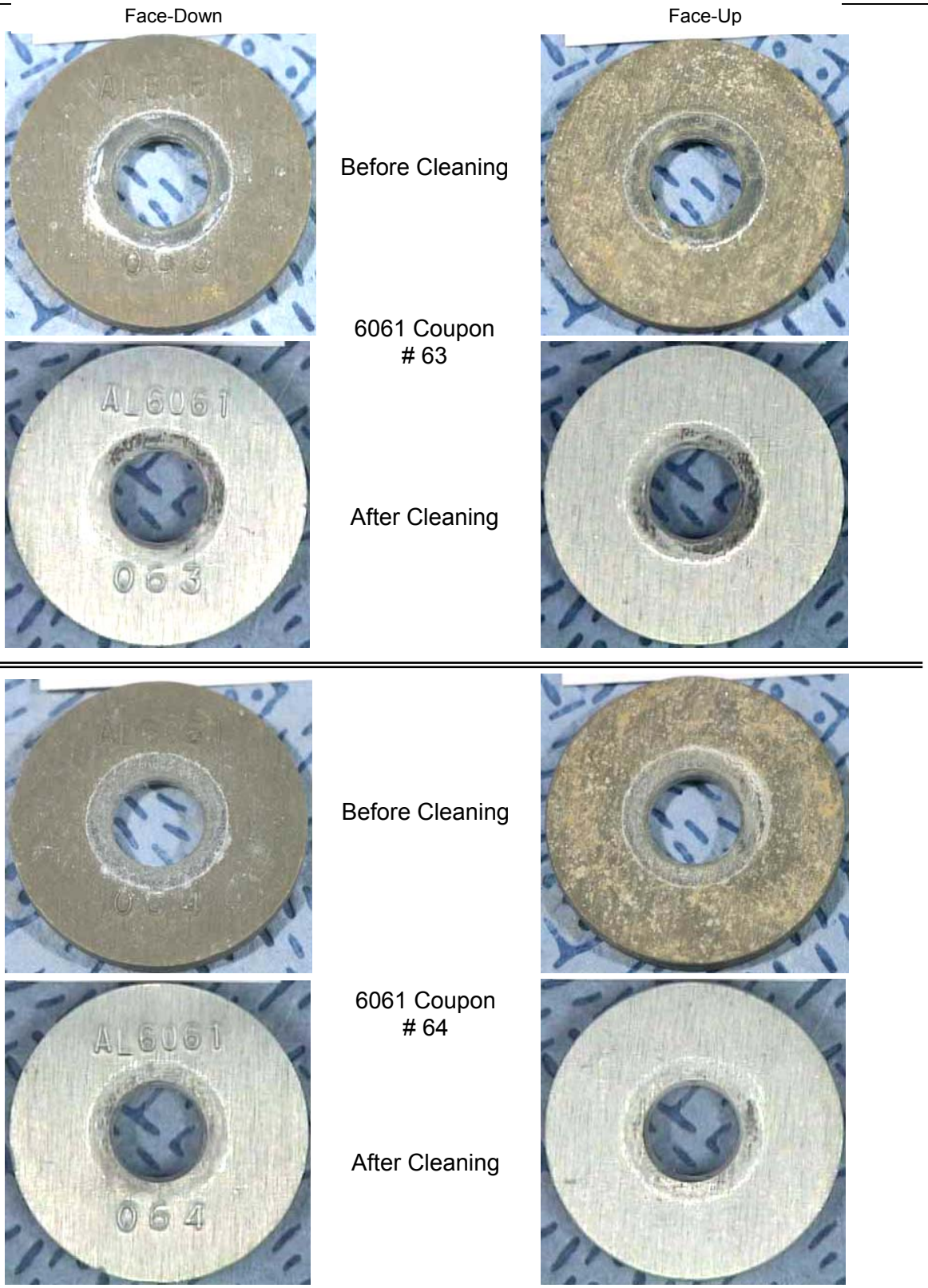


Figure A.9 Photos taken before and after cleaning of single 6061 coupons, #'s 63 and 64.

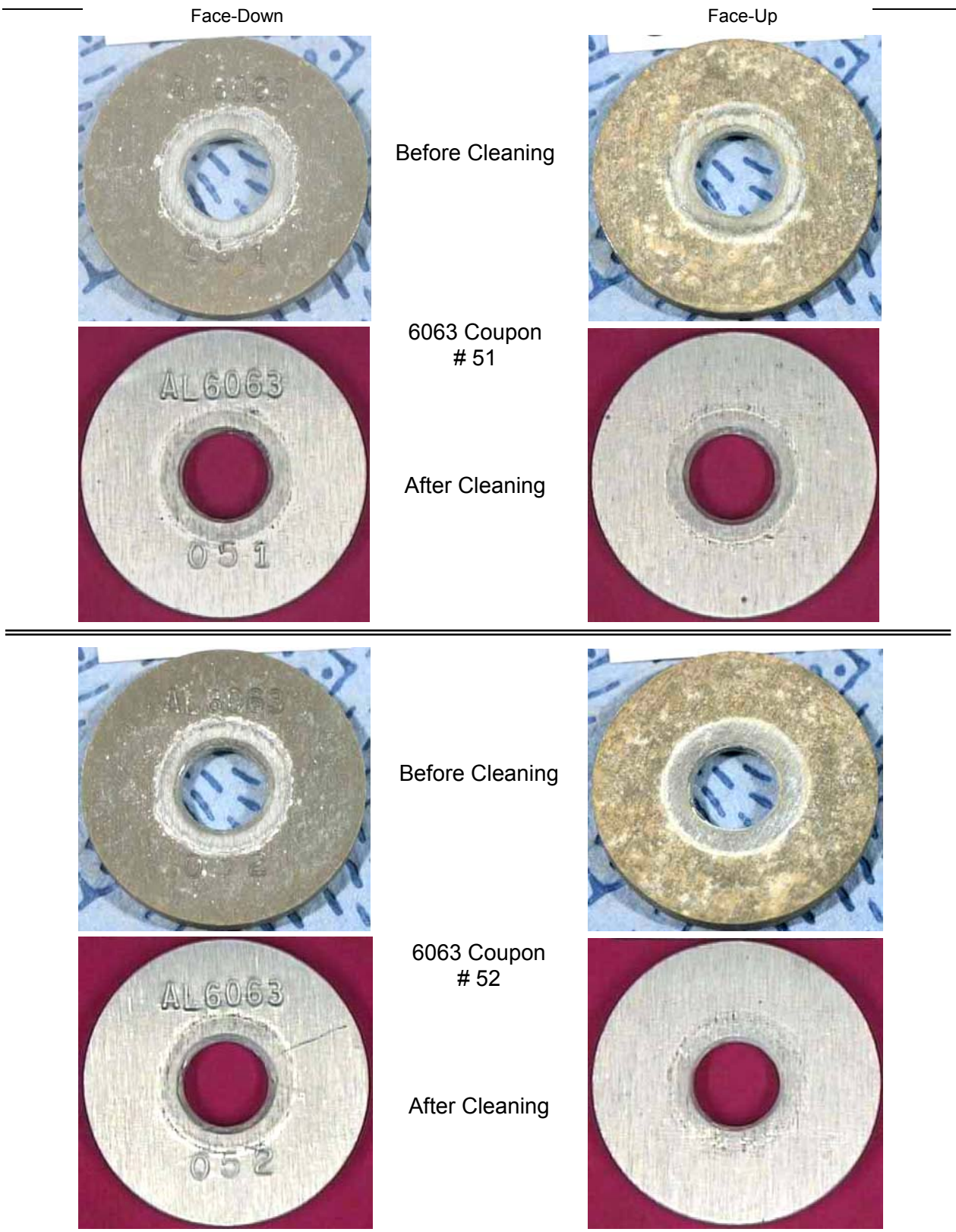


Figure A.10 Photos taken before and after cleaning of single 6063 coupons, #'s 51 and 52.

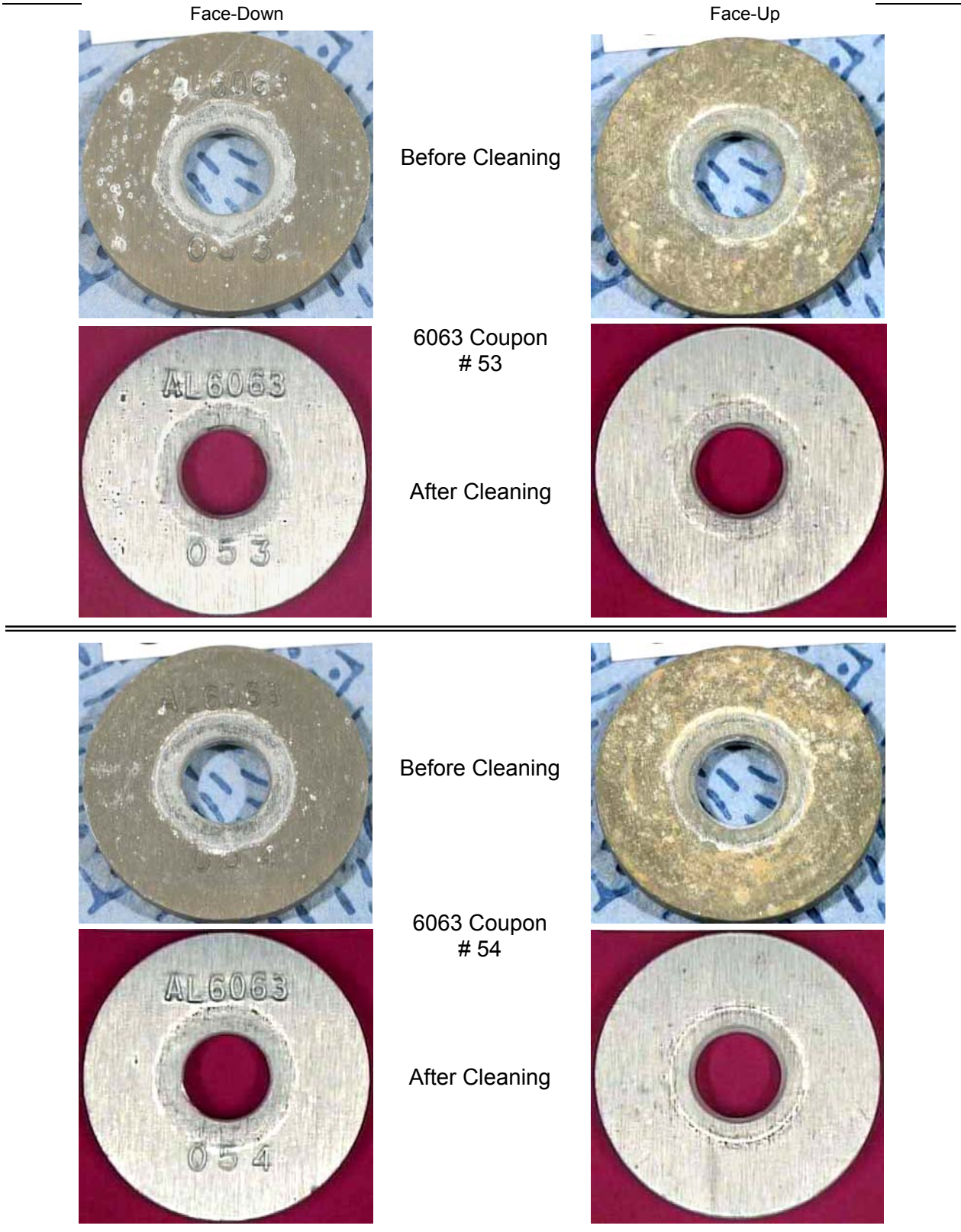


Figure A.11 Photos taken before and after cleaning of single 6063 coupons, #'s 53 and 54.

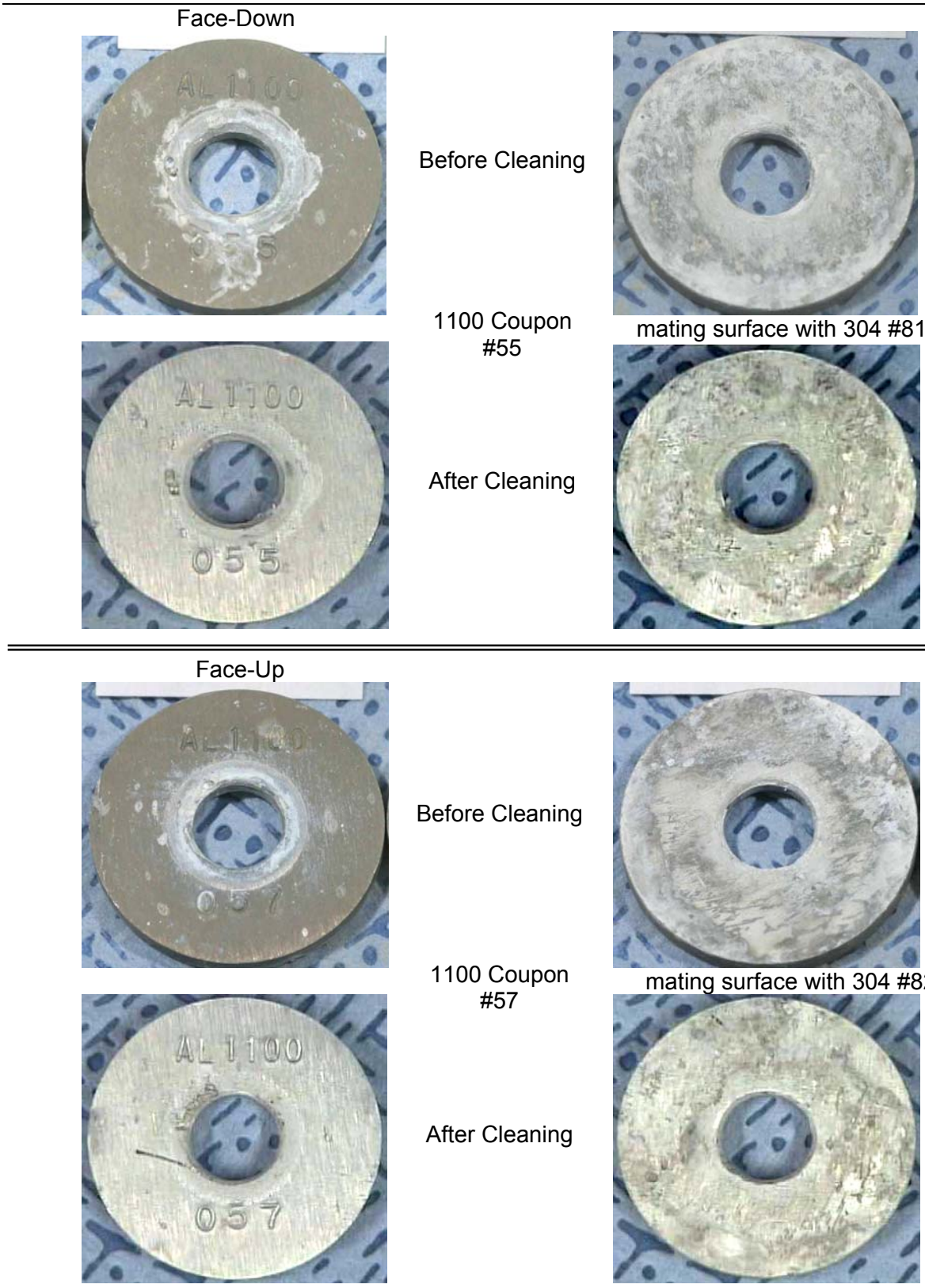


Figure A.12 Photos taken before and after cleaning of galvanic 1100 coupons, #'s 55 and 57, mated to 304 stainless steel.

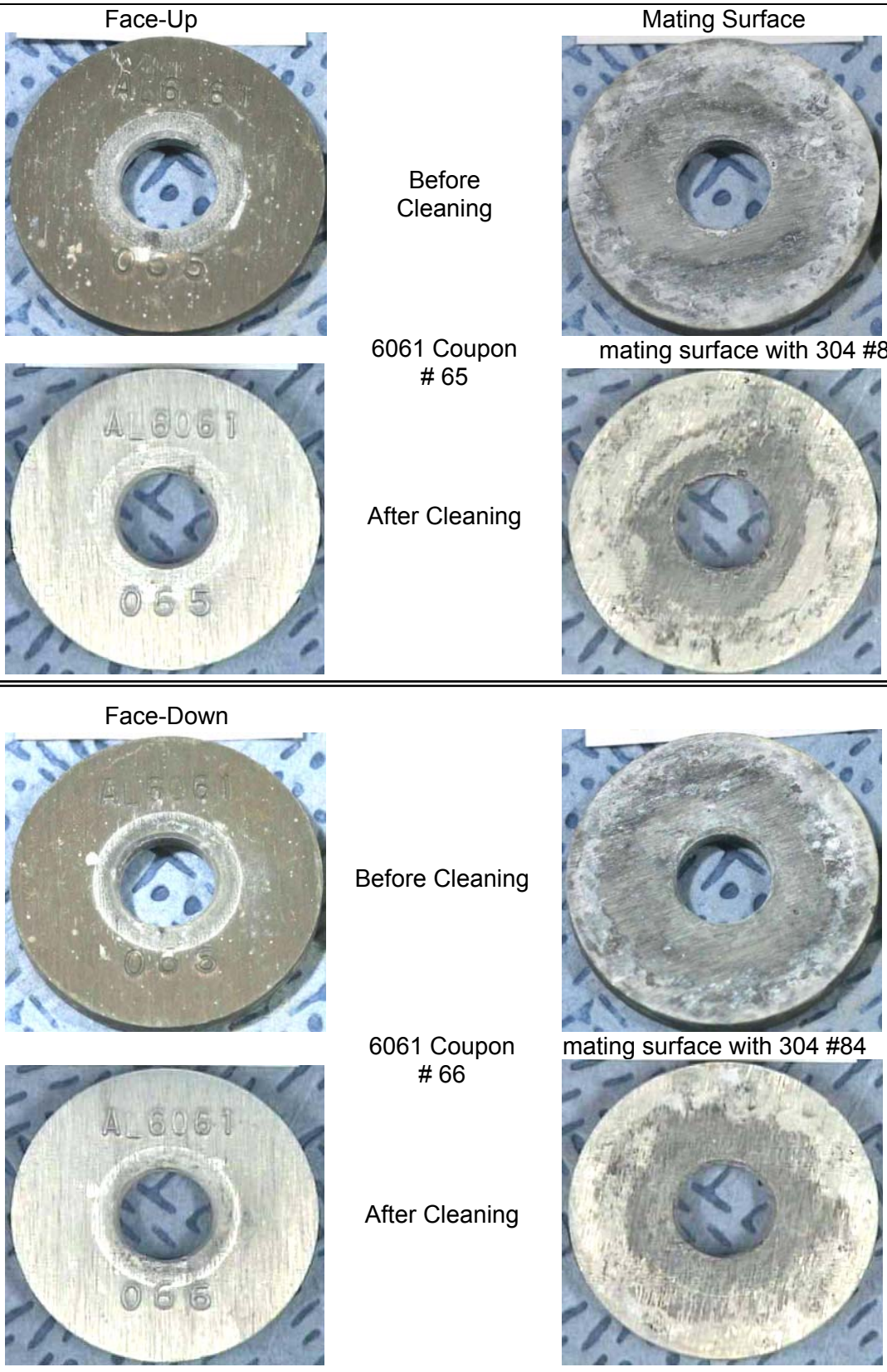


Figure A.13 Photos taken before and after cleaning of galvanic 6061coupons, #'s 65 and 66, mated to 304 stainless steel.

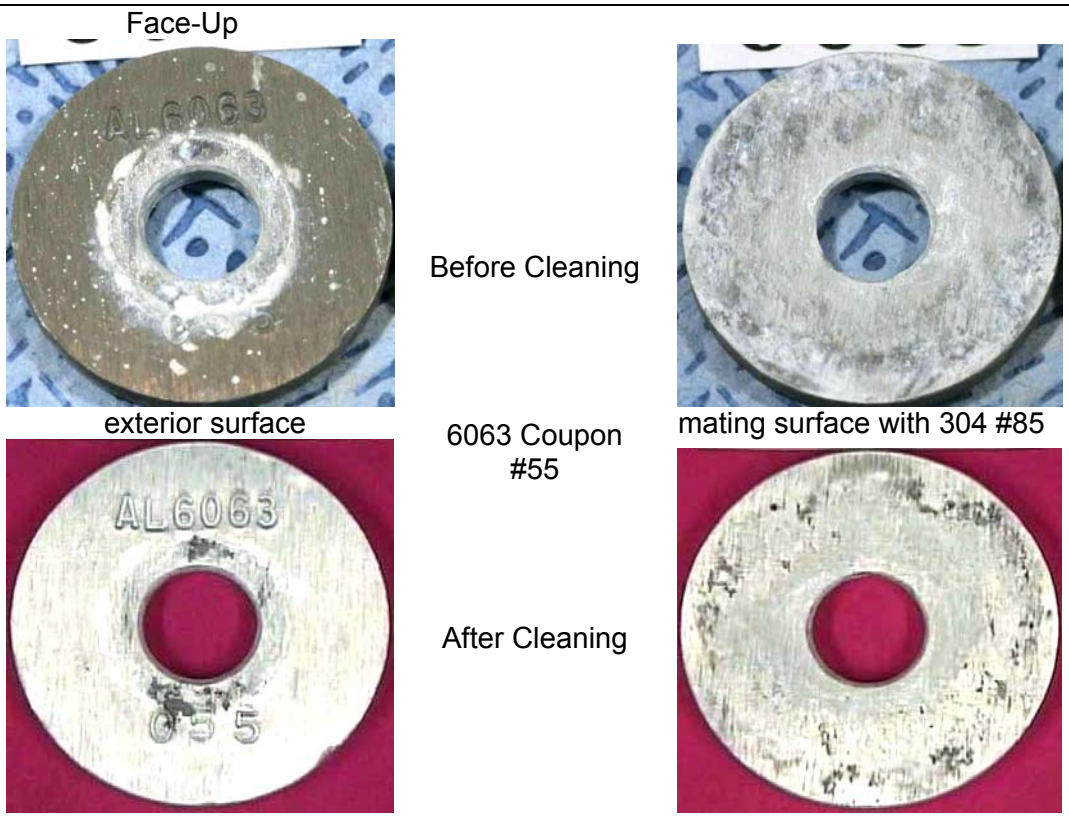


Figure A.14 Photos taken before and after cleaning of galvanic 6063 coupons, #'s 55 and 56, mated to 304 stainless steel.


Figure A.15 Photos taken before and after cleaning of crevice (two of the same alloy mated together) coupons (Al 1100 #'s 56 and 58.


Figure A.16 Photos taken before and after cleaning of crevice (two of the same alloy mated together) coupons (Al 1100 #'s 59 and 60)..


Figure A.17 Photos taken before and after cleaning of crevice (two of the same alloy mated together) coupons (Al 6061 #'s 67 and 68).


Figure A.18 Photos taken before and after cleaning of crevice (two of the same alloy mated together) coupons (Al 6061 #'s 69 and 70).

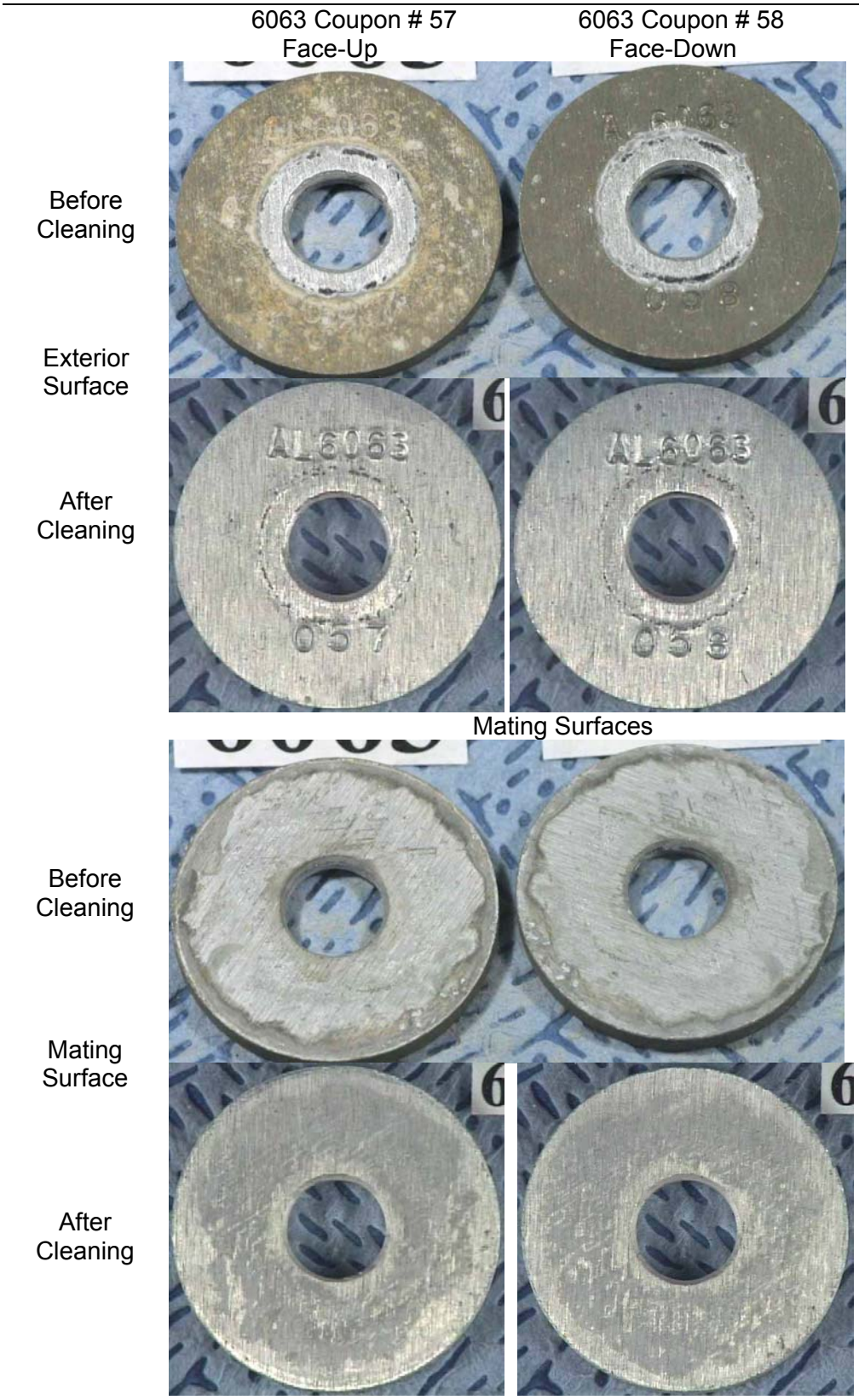


Figure A.19 Photos taken before and after cleaning of crevice (two of the same alloy mated together) coupons (Al 6063 #'s 57 and 58).

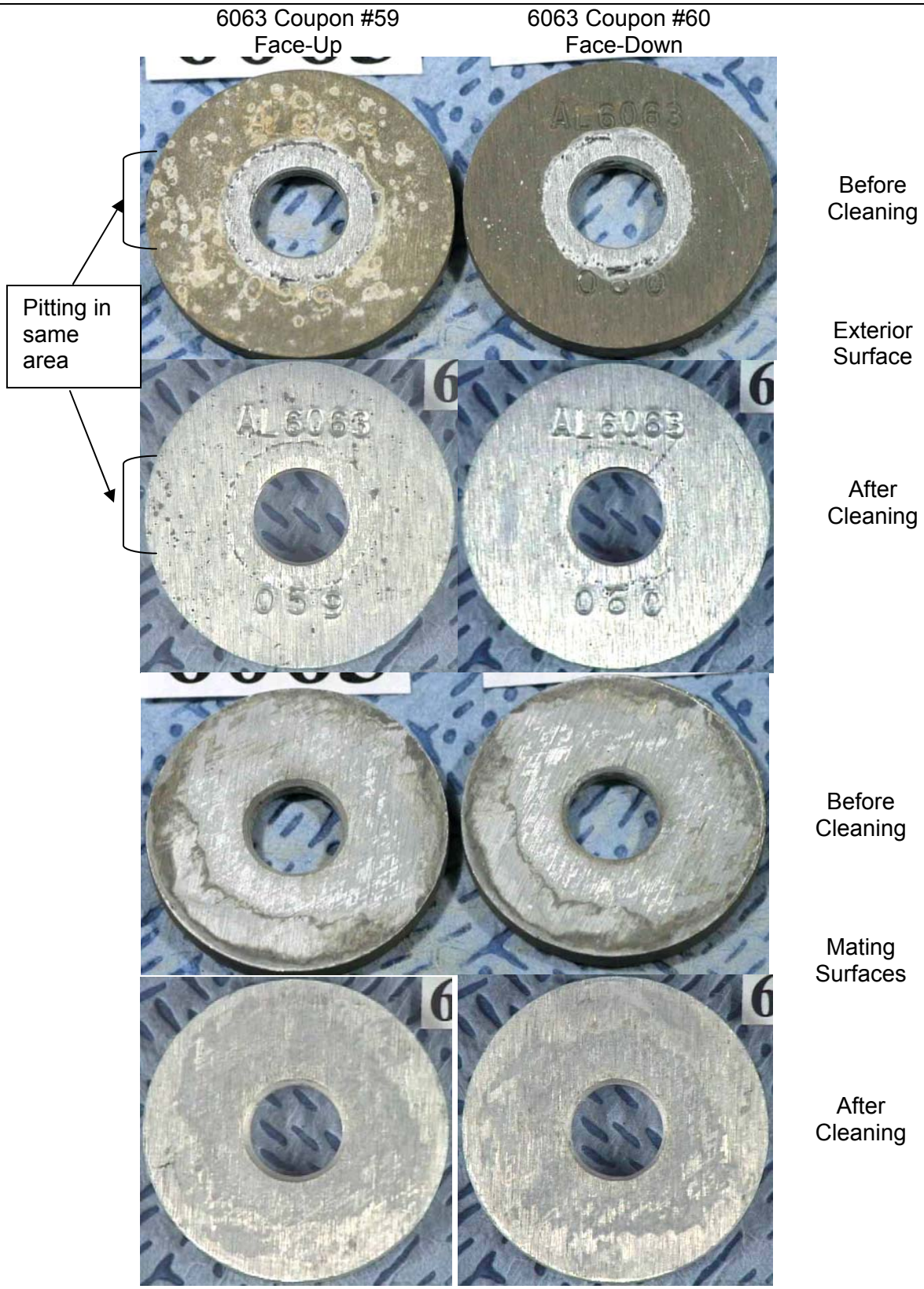


Figure A.20 Photos taken before and after cleaning of crevice (two of the same alloy mated together) coupon surfaces (Al 6063 #'s 57 and 58).

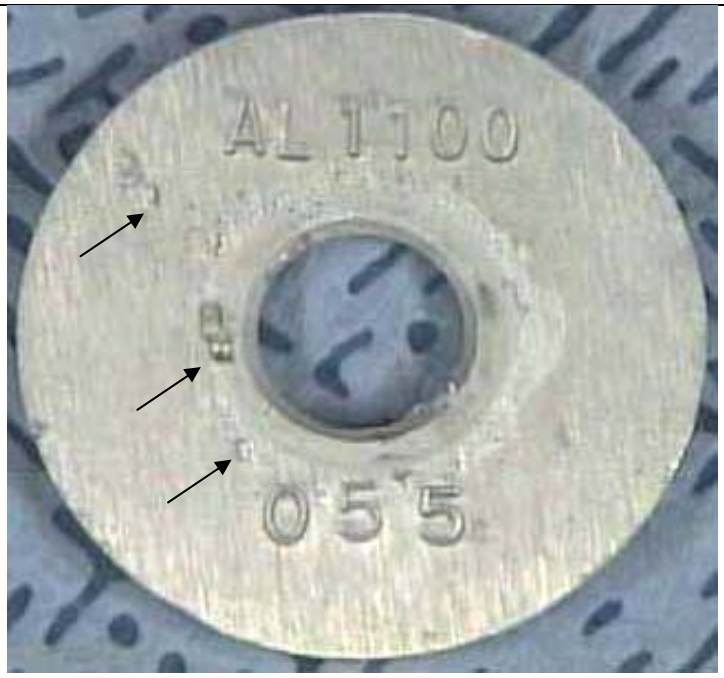


Figure A.21 Pits shown in Face-Down orientation of Al 1100 #055 coupon

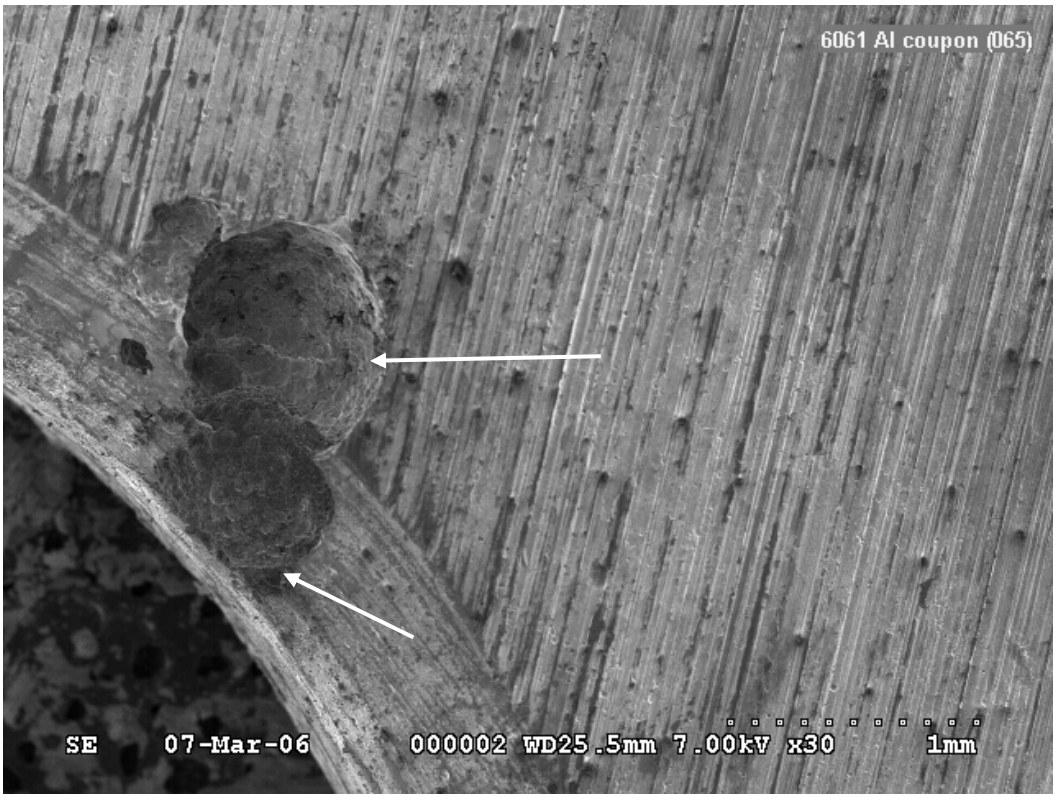


Figure A.22 Pits shown in crevice area beneath PTFE washer on Face-Up side of Al 6061 #065 coupon. The surface of this coupon is shown in Figure A.13.

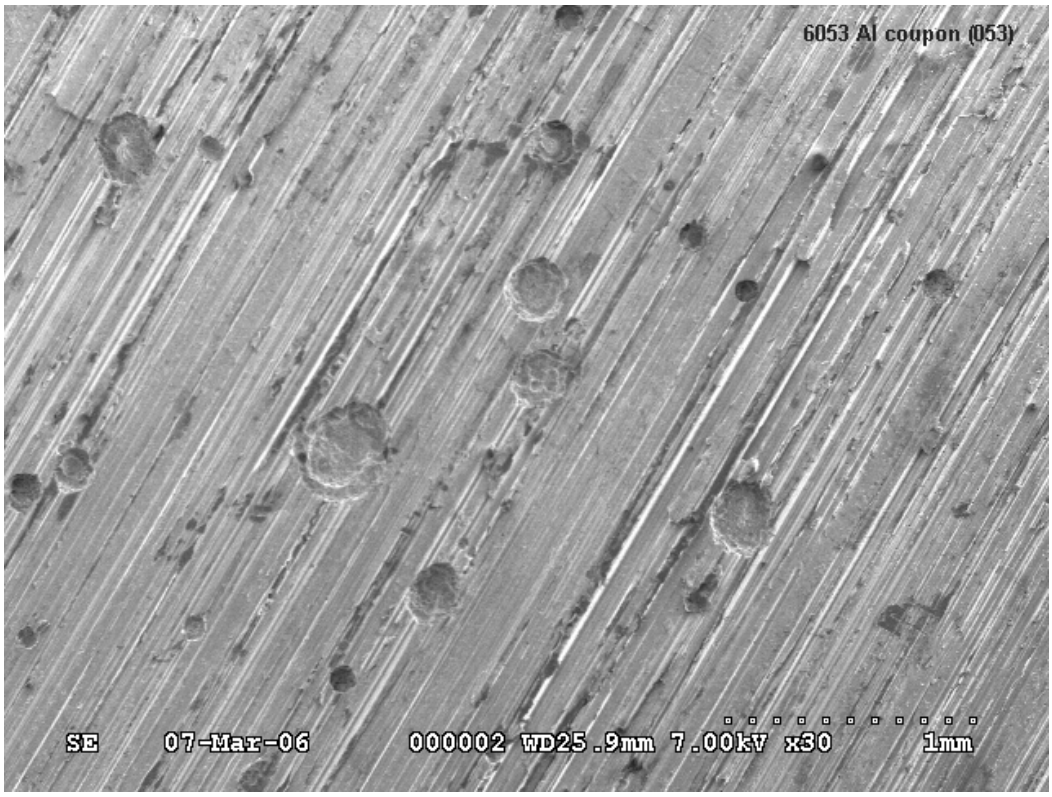


Figure A.23 Pits shown on open surface of a single Al 6063 #053 coupon. This surface was in the Face-Up position and is shown in Figure A.6.

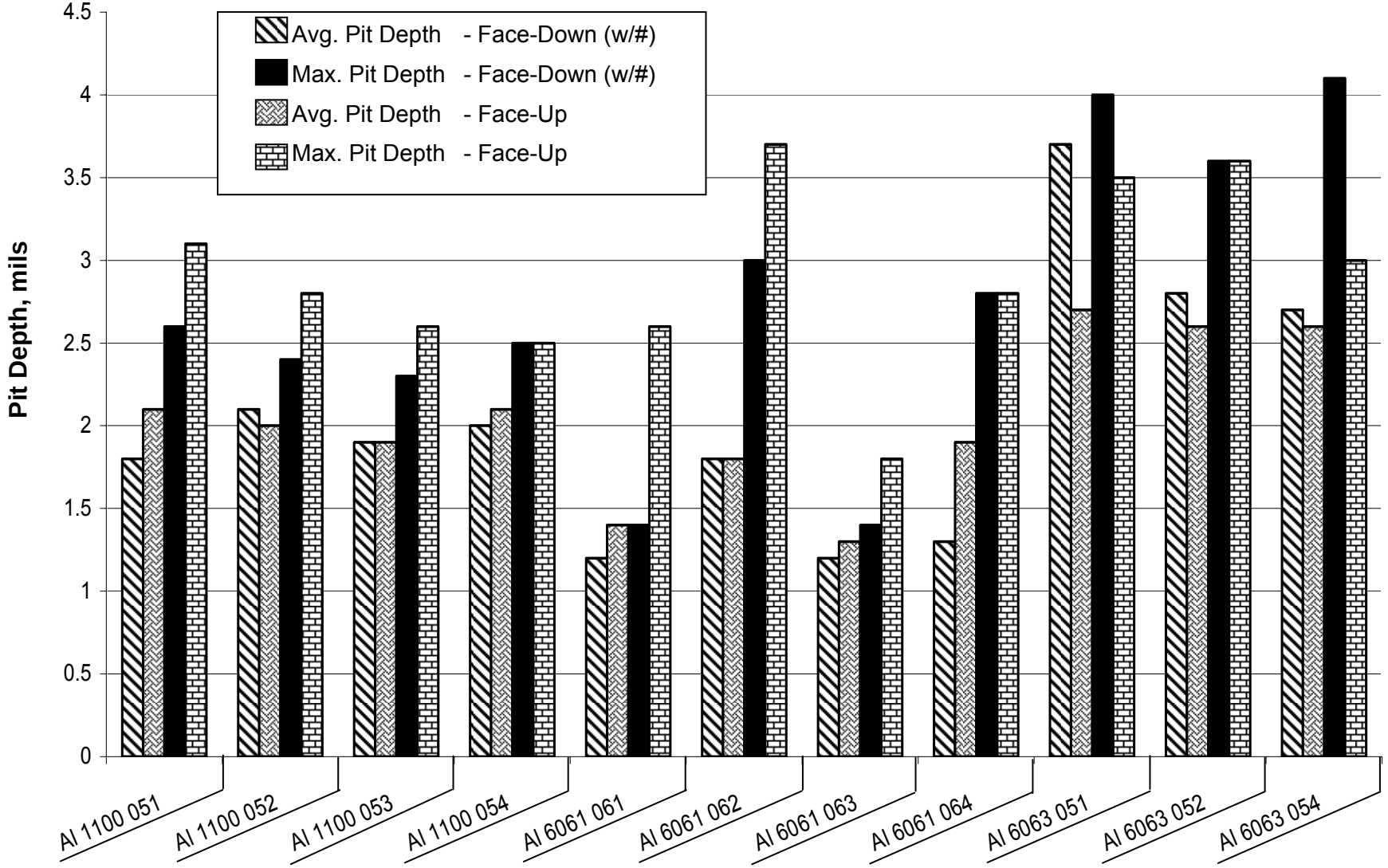


Figure A.24 Effect of aluminum alloy type and orientation on pit depths. Note: In this figure, the numbered (#) side was always face down in the basin.

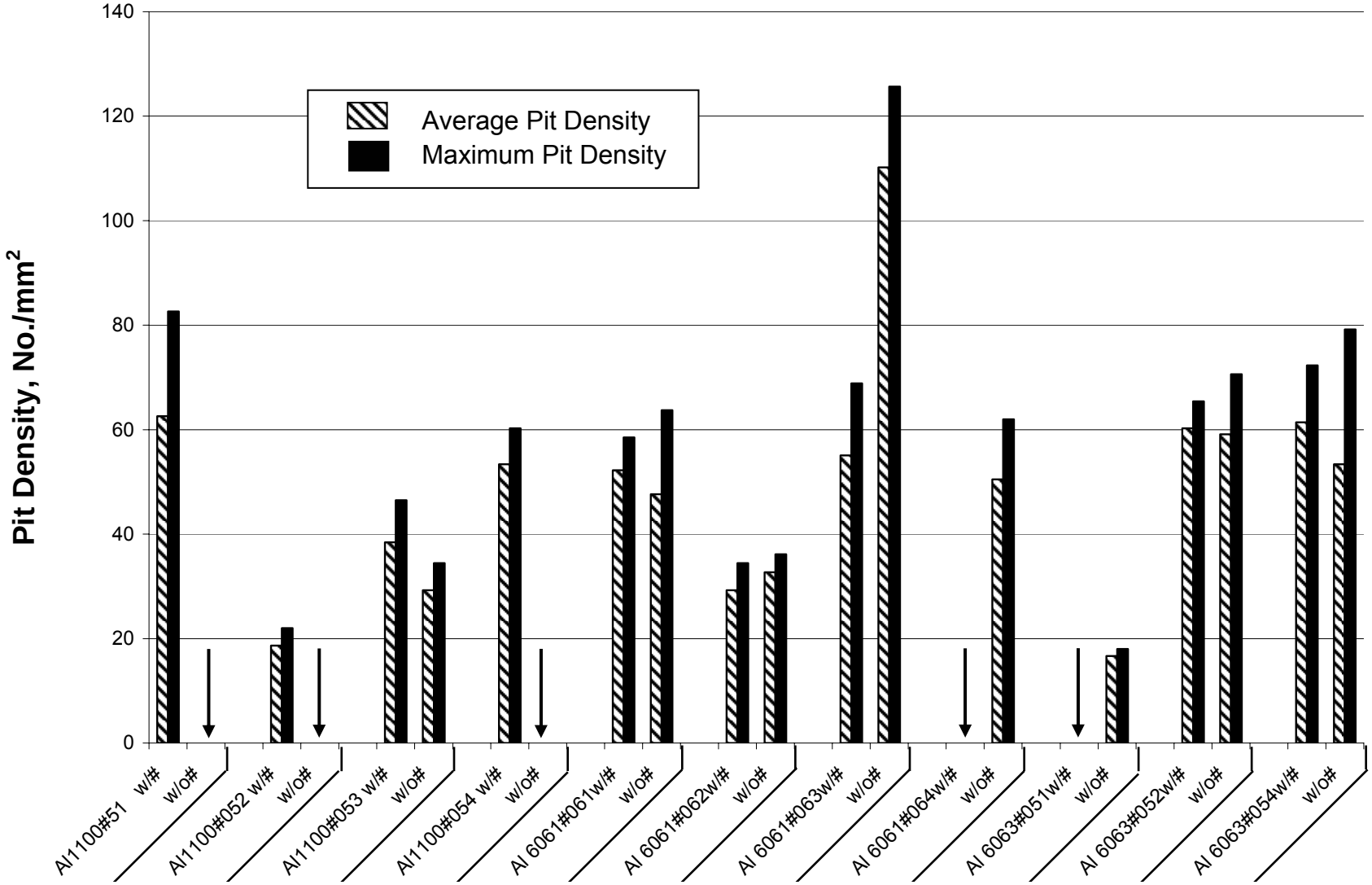


Figure A.25 Effect of aluminum alloy type and orientation on pit densities. Data for both sides of the coupon are shown: w/# is side facing down in the basin while w/o# is side facing up. Arrows indicate very low pit densities (< 5 pits/mm$^2$).

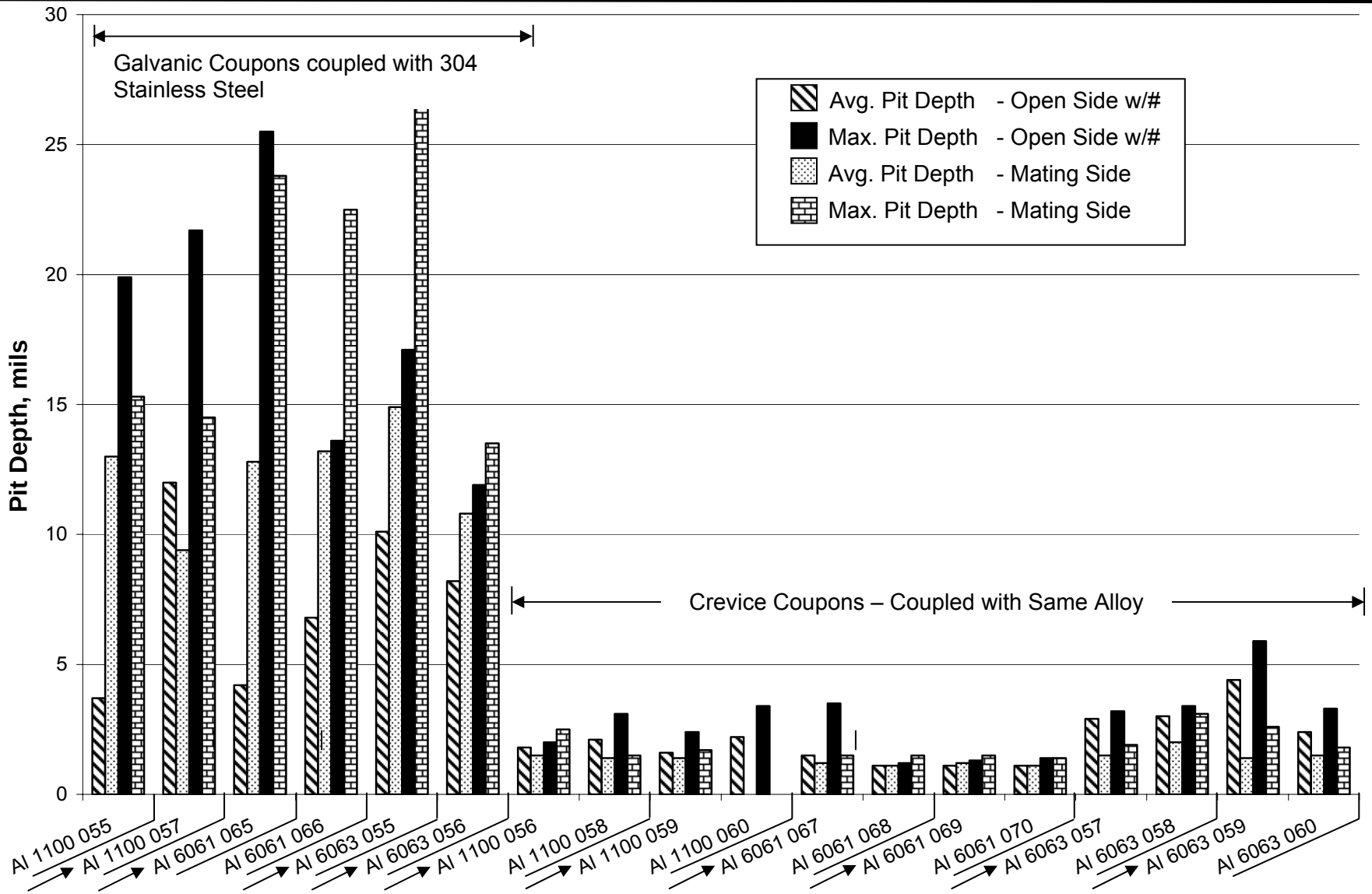


Figure A.26 Effect of coupon type (galvanic and crevice) and orientation on pit depths. Arrows indicate # side of coupon in Face-Up position.

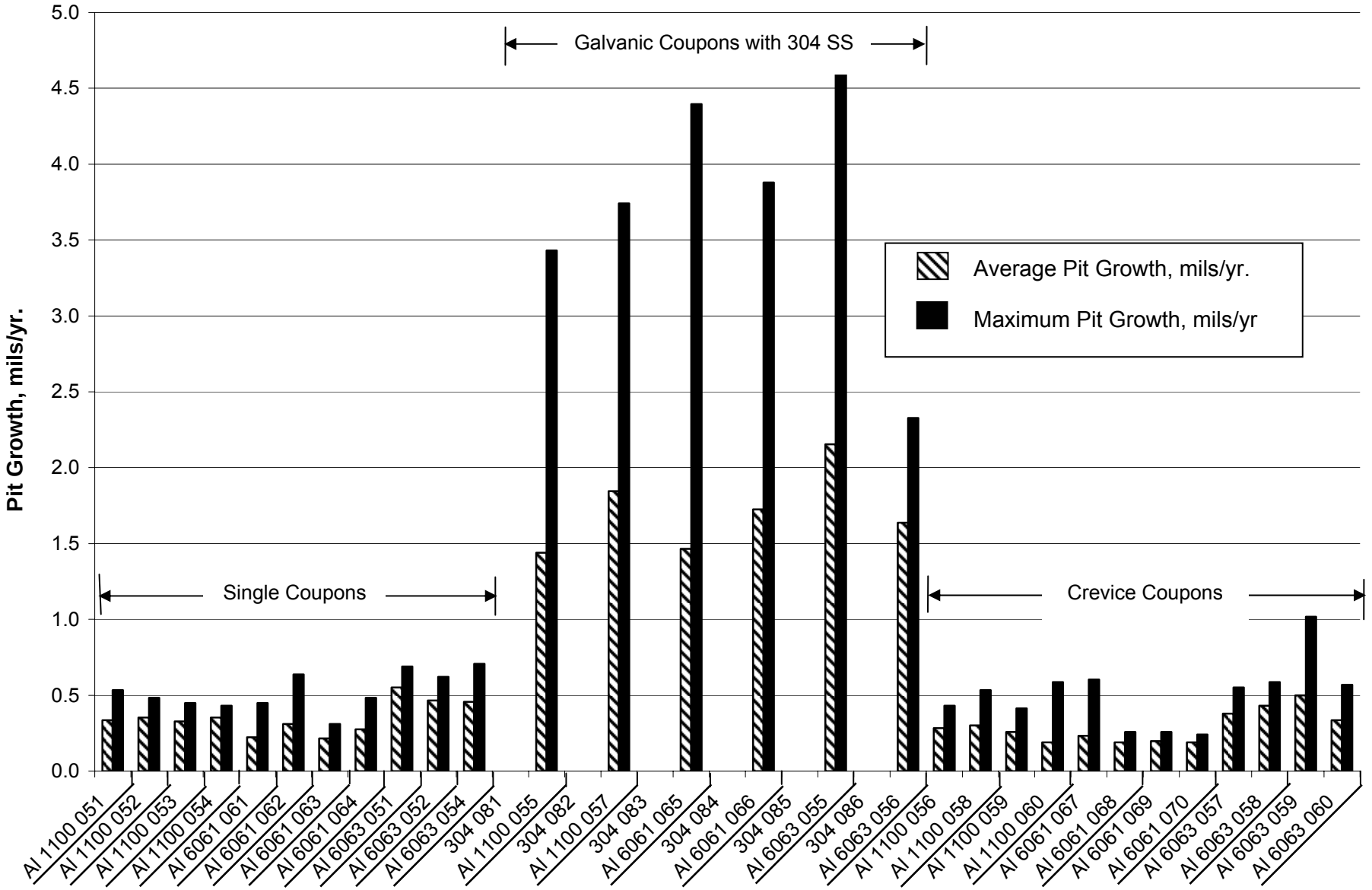


Figure A.27 Effect of coupon types and alloy on pit growth.

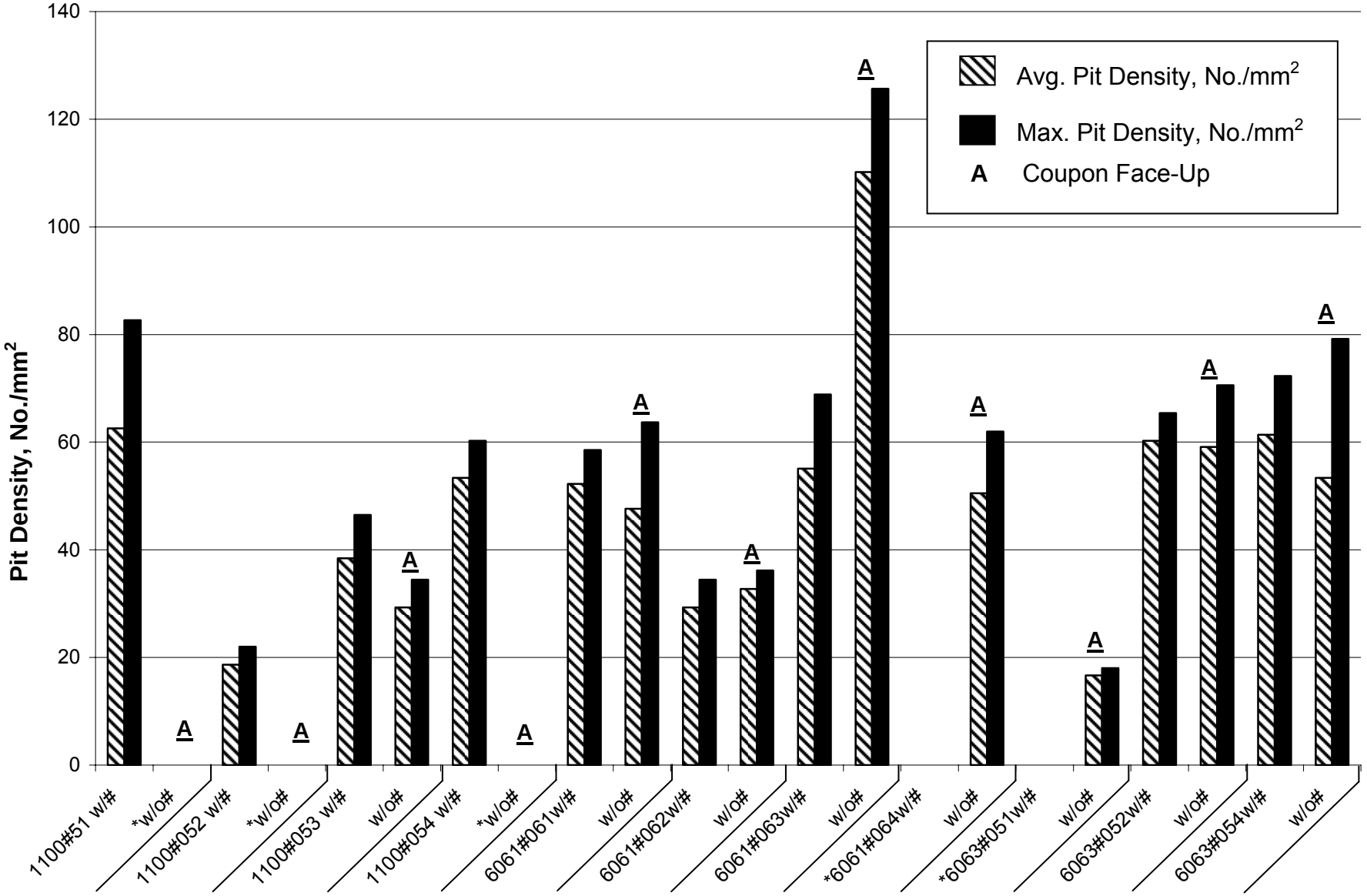


Figure A.28 Effect of coupon type, alloy type and surface orientation on pit density. The asterisk indicates that surface displayed less than 50 pits.

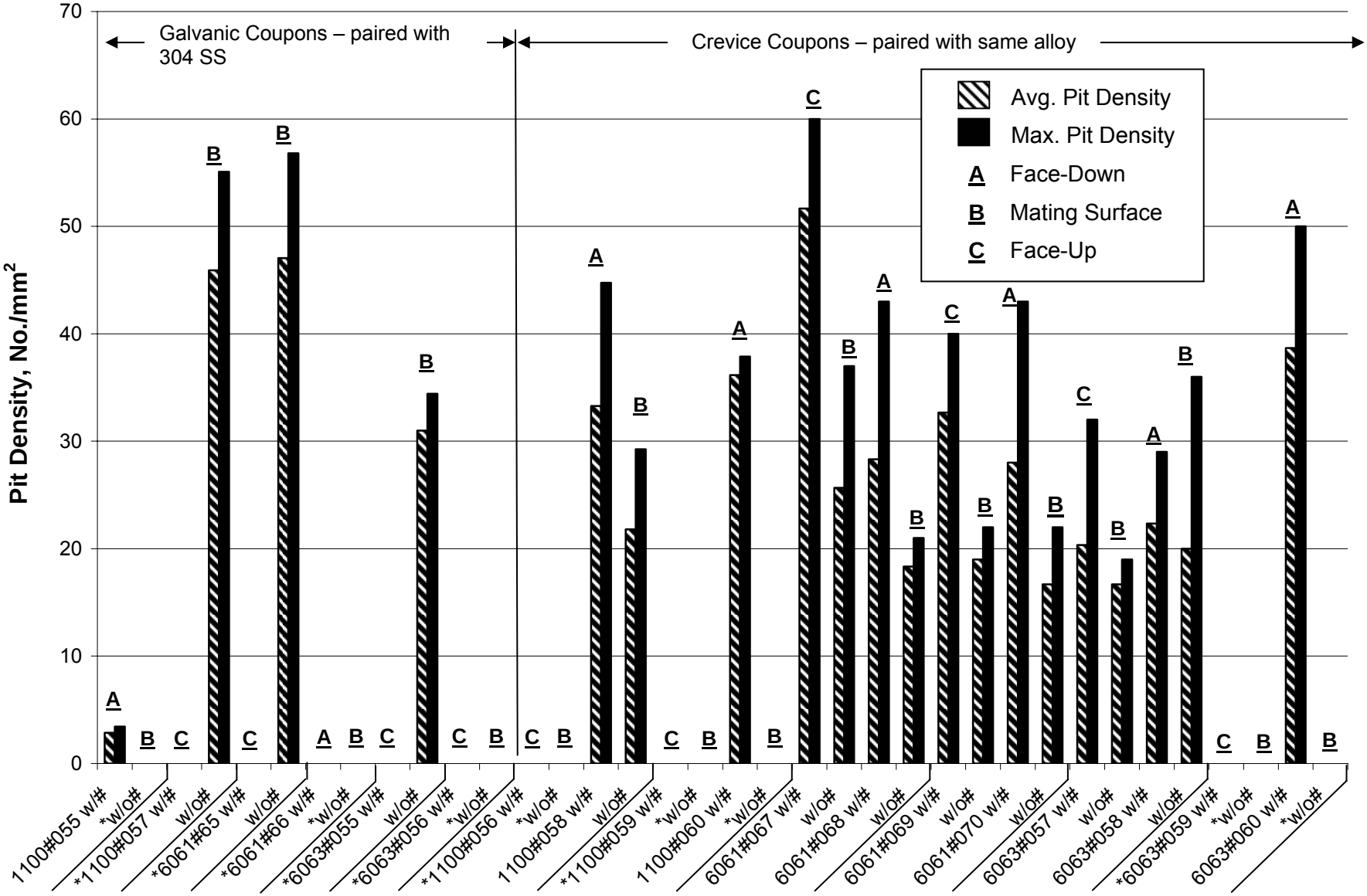


Figure A.29 Effect of galvanic or crevice pairs, alloy type, and orientation on pit density. Alloy coupon surfaces denoted with an asterisk displayed a total number of pits in three separate 0.58 $mm^2$ areas to be < 50.

# Appendix B

## Coupon Photos and Data Graphs from FY2006 Corrosion Surveillance

### LIST OF FIGURES


Figure B.1 As-received 2006 coupon string from L-Basin.

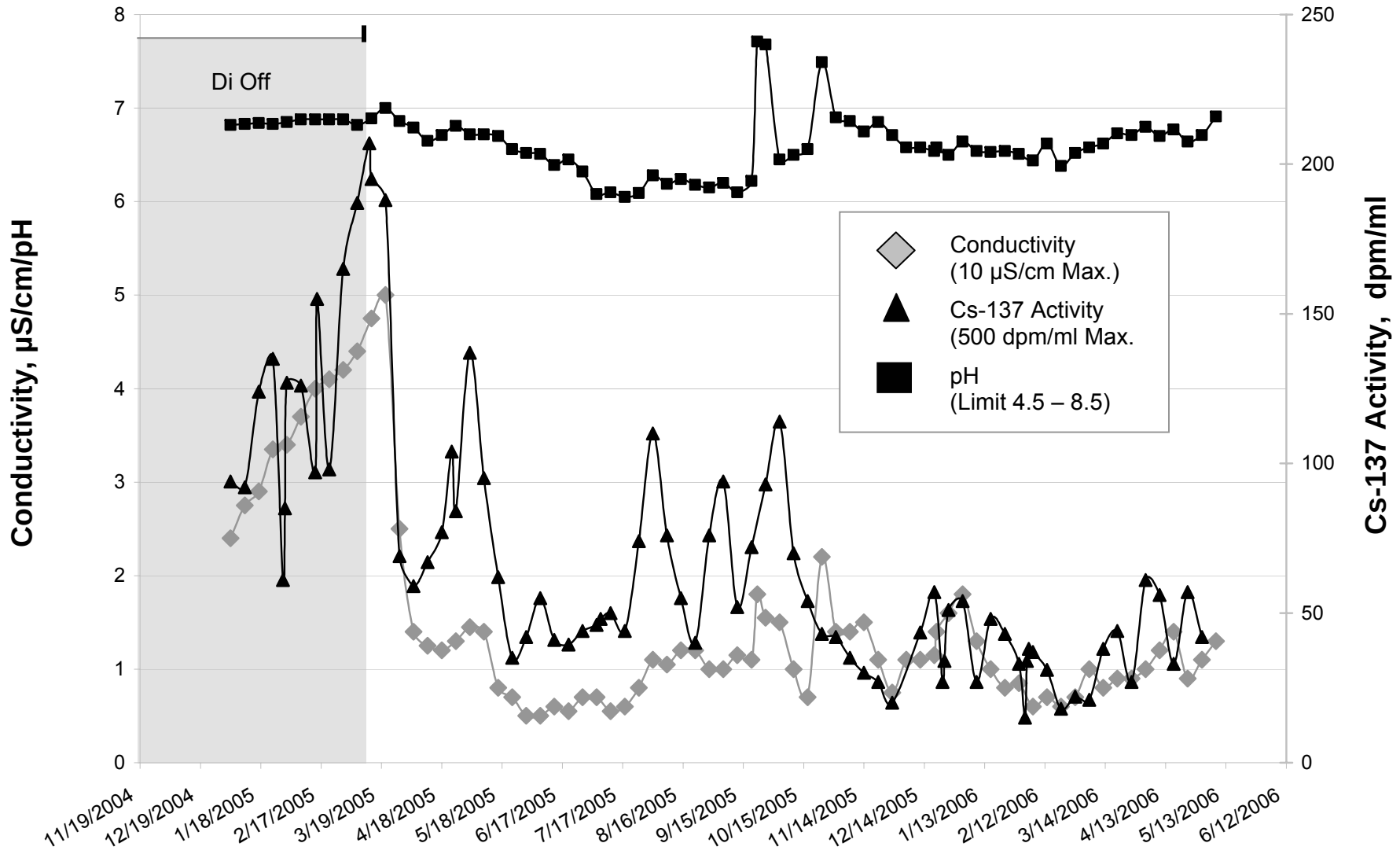


Figure B.2 Time dependent conductivity, pH, Cs-137 in L-Basin during the period January 2005 to May 2006.

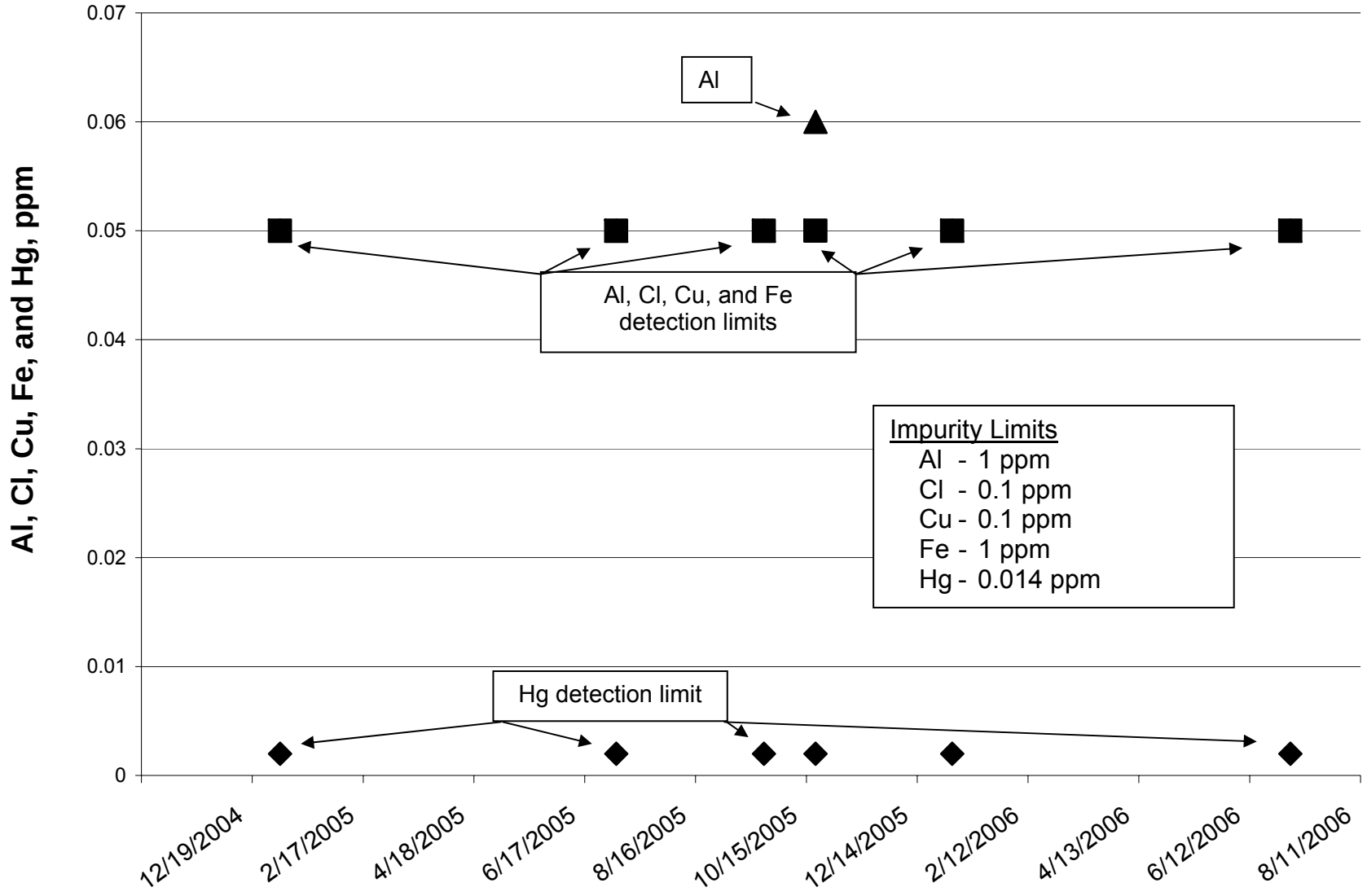


Figure B.3 Time dependent impurity levels in L-Basin during the period January 2005 to July 2006. All but one data point is below the detectible limits. Elemental Aluminum was detected at 0.06 ppm on 10/20/2005 but is still well below the limit of 1 ppm.

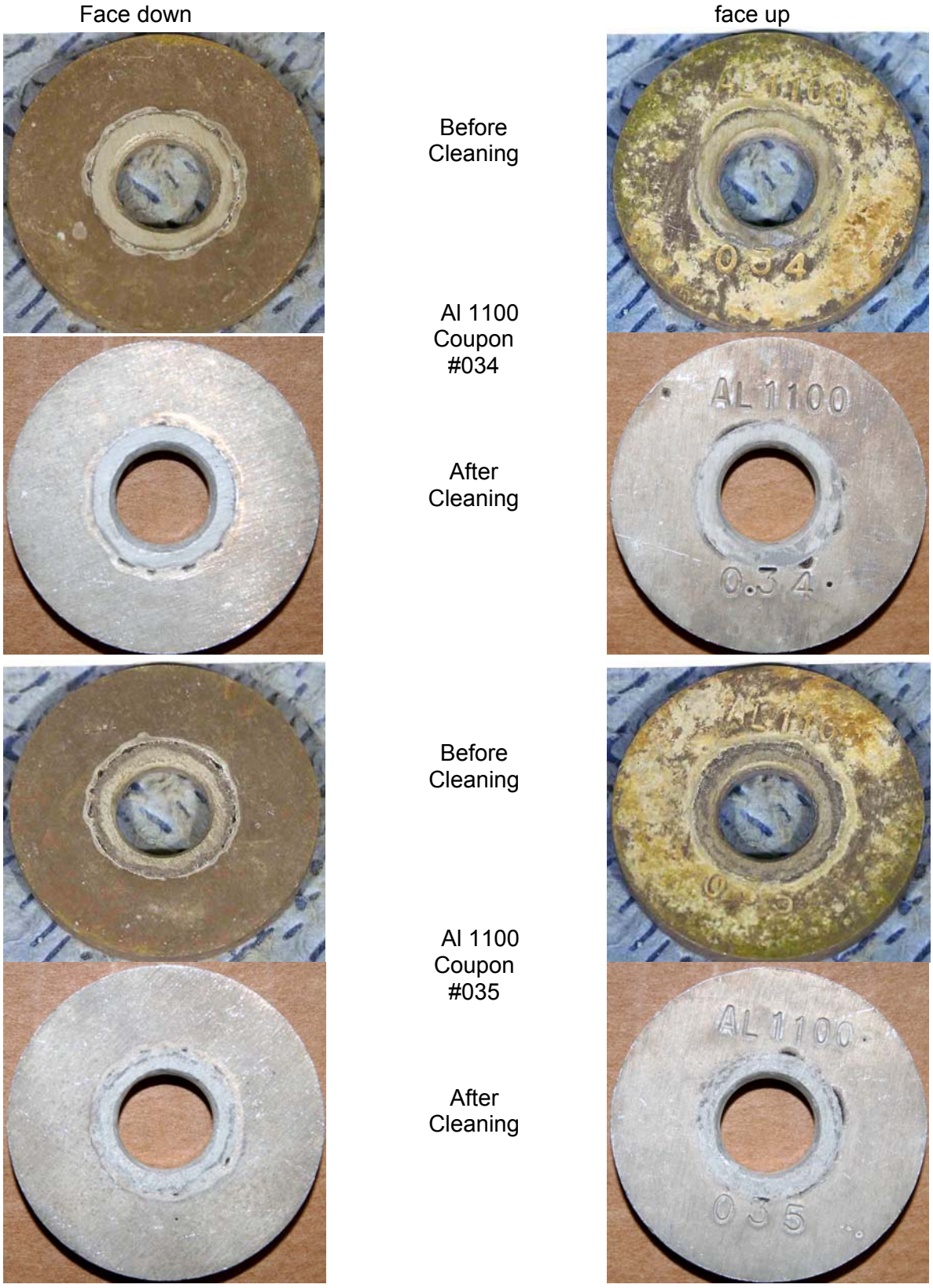


Figure B.4 Photos taken before and after cleaning of single 1100 coupons, #'s 034 and 035.

Face down

Face-Up

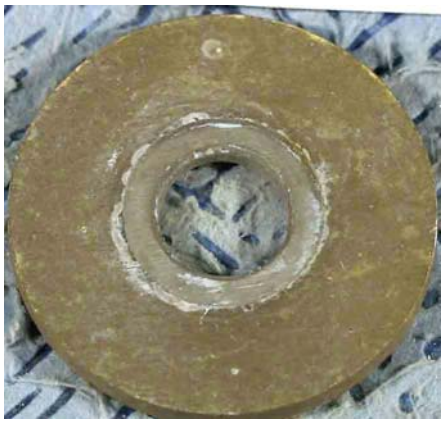

Al 1100
Coupon
#036
Before
Cleaning

Before
Cleaning


Al 1100
Coupon
#037

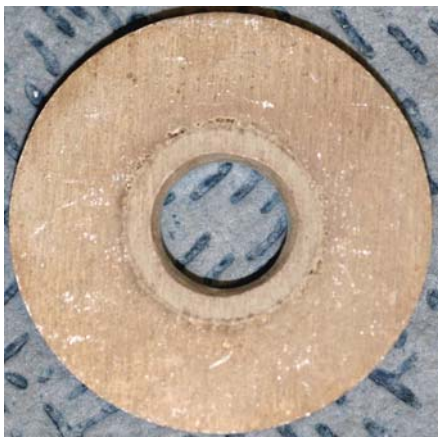

After
Cleaning


Figure B.5 Photos taken before and after cleaning of single 1100 coupons, #'s 036 and 037. Coupon #036 was sectioned for surface analysis in the SEM and never cleaned.

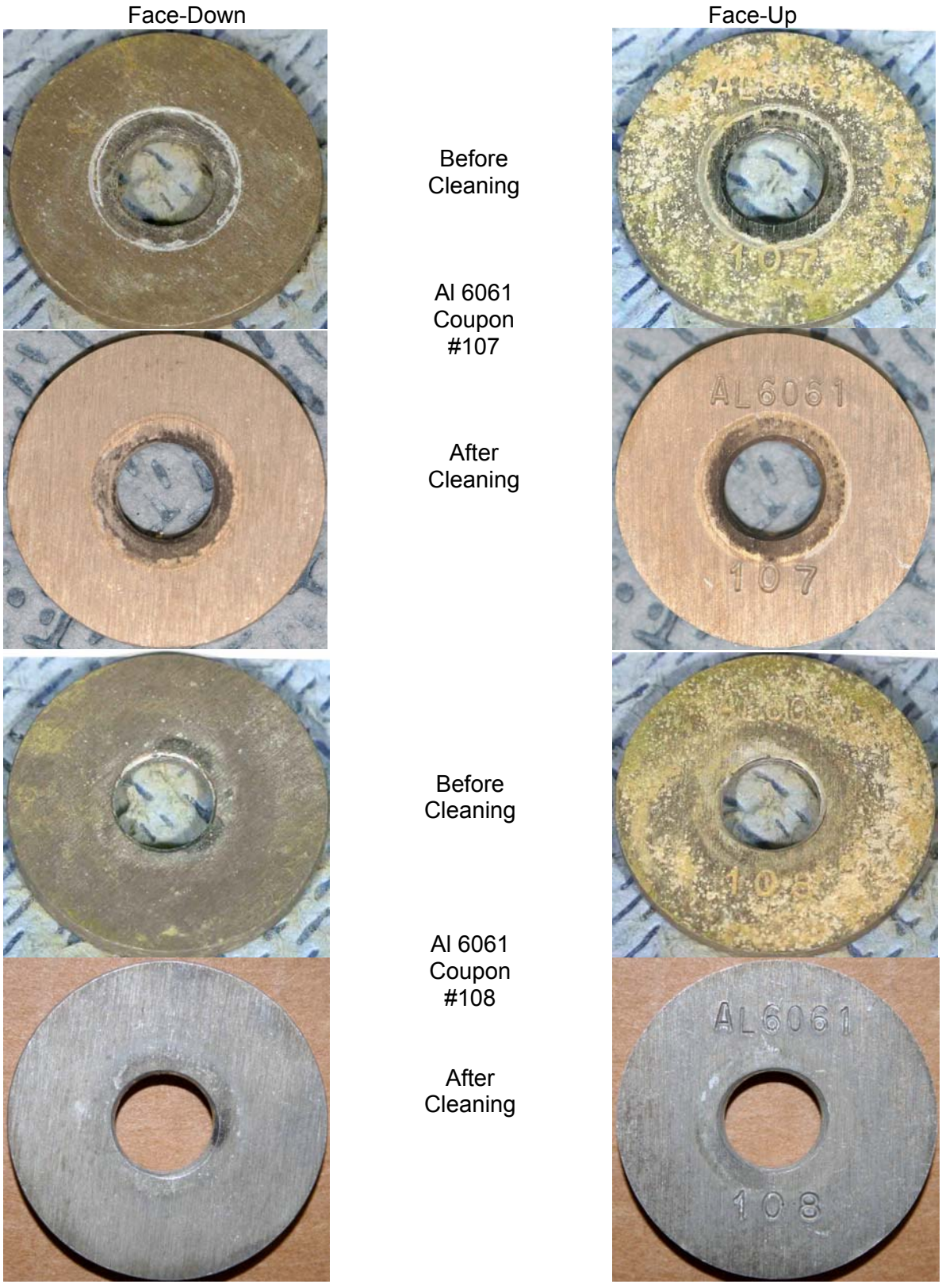


Figure B.6 Photos taken before and after cleaning of single 6061 coupons, #'s 107 and 108.

**Face-Down**

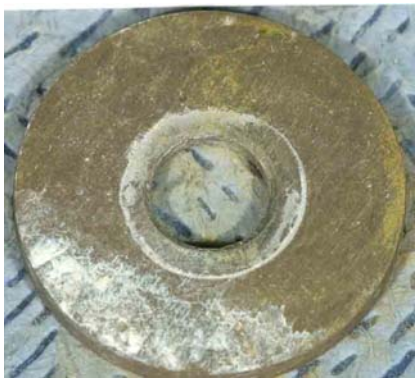

Al 6061
Coupon
#109

Before
Cleaning

**Face-Up**

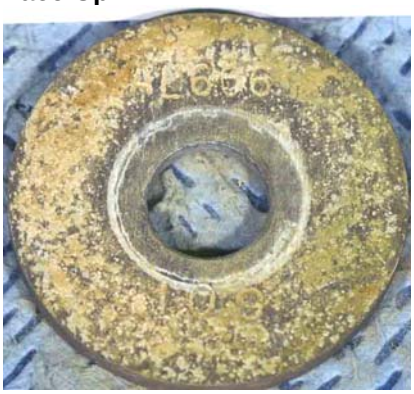

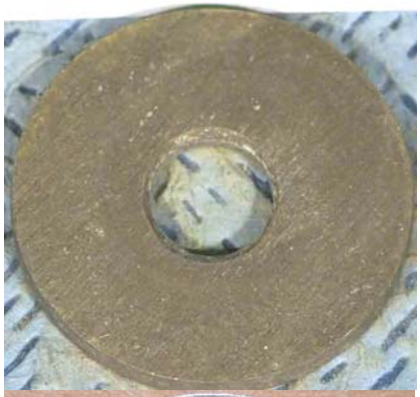

Before
Cleaning

Al 6061
Coupon
#110

After
Cleaning


Figure B.7 Photos taken before and after cleaning of single 6061 coupons, #'s 109 and 110. Coupon #109 was contaminated during surface analysis in the SEM and never cleaned.

.

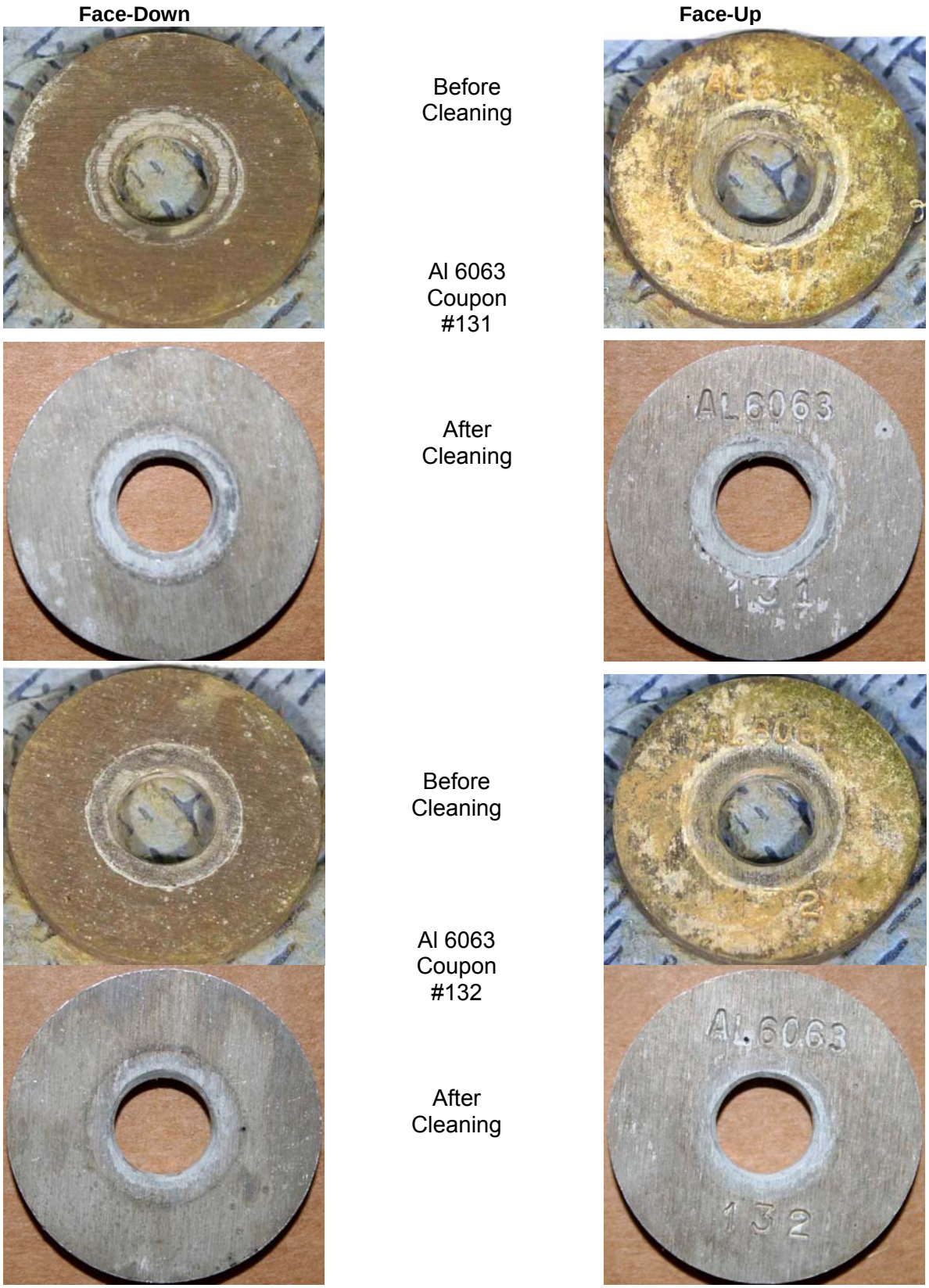


Figure B.8 Photos taken before and after cleaning of single 6063 coupons, #'s 131 and 132.

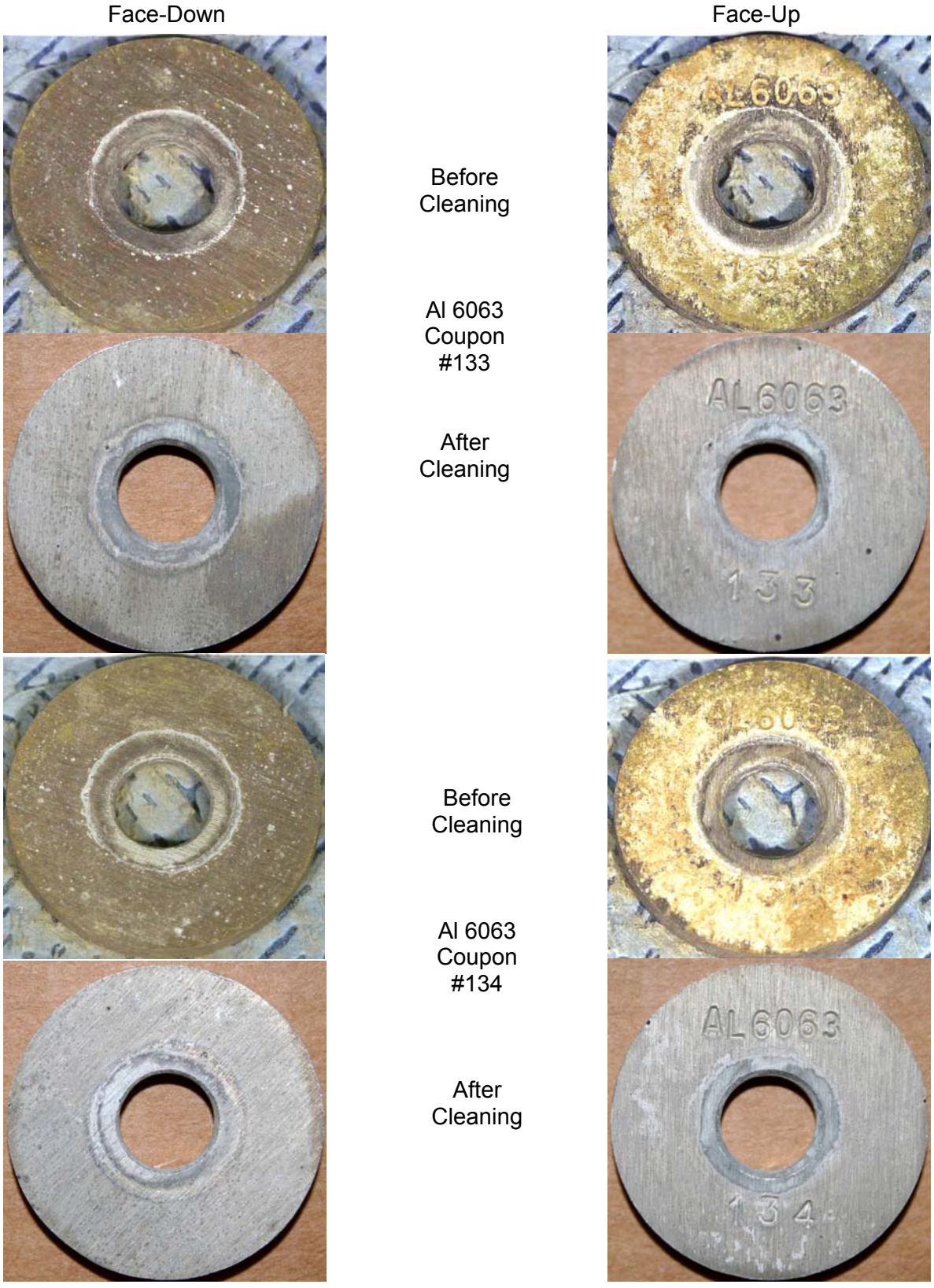


Figure B.9 Photos taken before and after cleaning of single 6063 coupons, #'s 133 and 134.


Figure B.10 Photos taken before and after cleaning of crevice (two of the same alloy mated together) coupons (Al 1100 #'s 21 and 22).

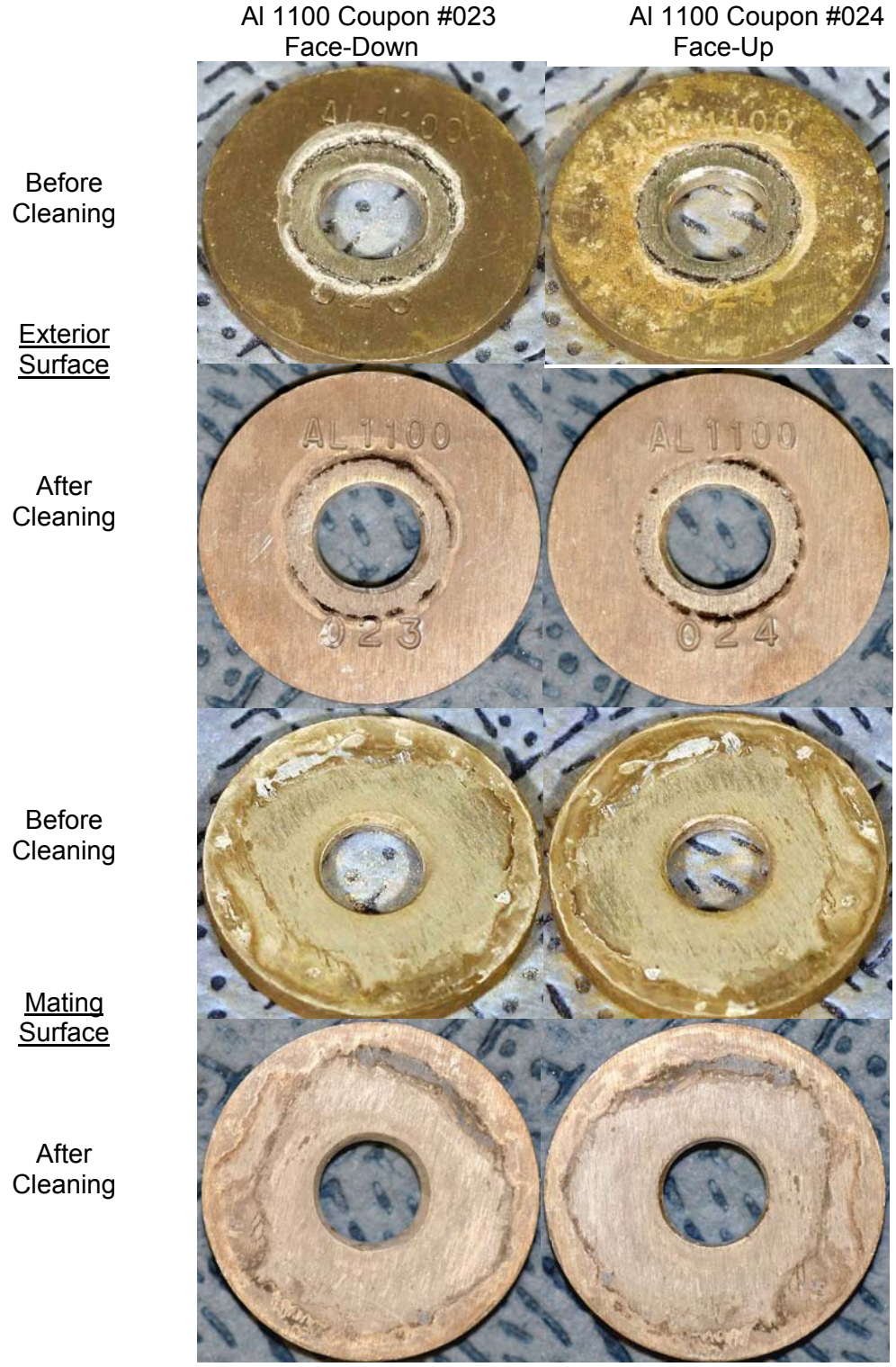


Figure B.11 Photos taken before and after cleaning of crevice (two of the same alloy mated together) coupons (Al 1100 #'s 23 and 24).

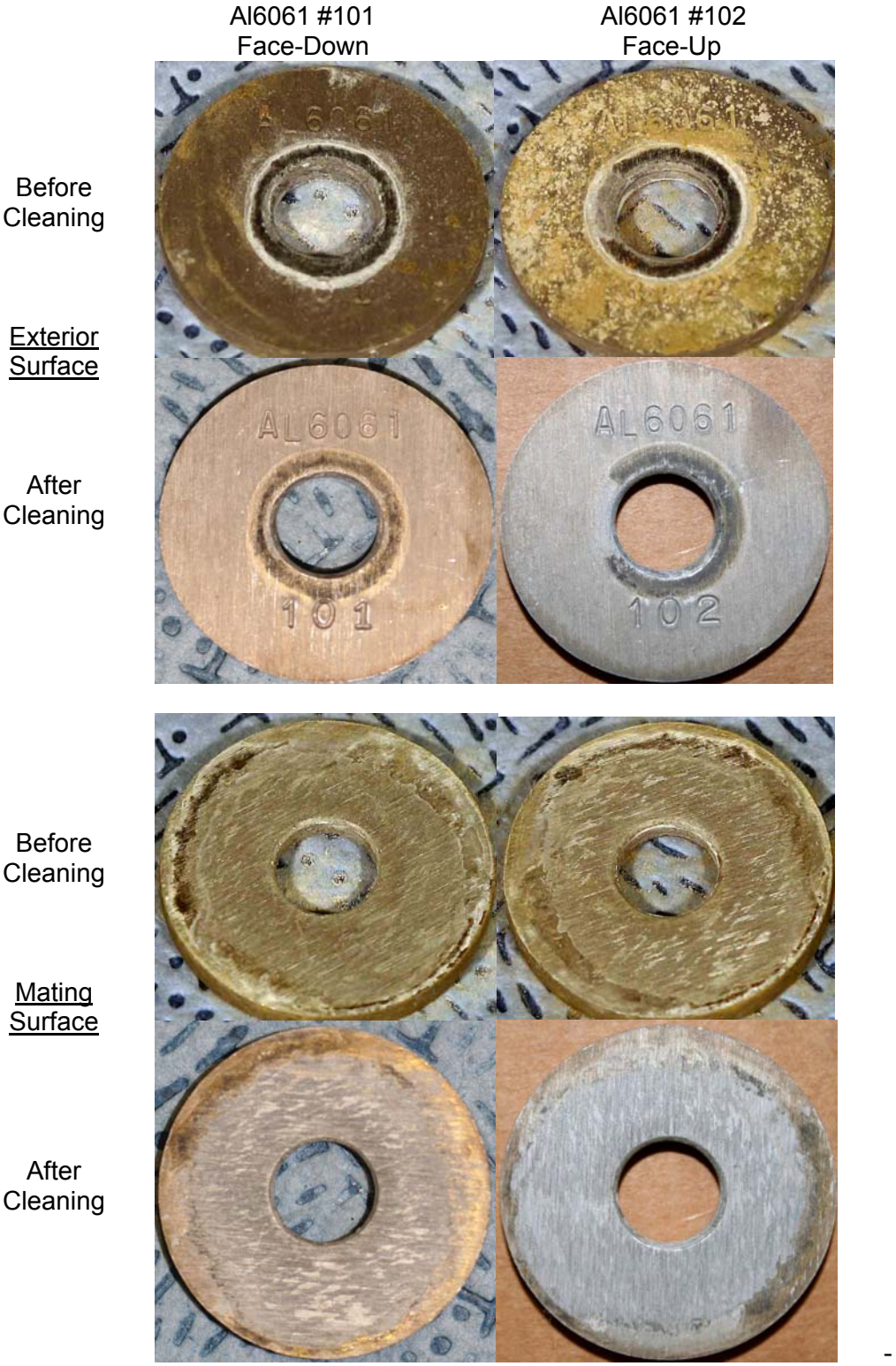


Figure B.12 Photos taken before and after cleaning of crevice (two of the same alloy mated together) coupons (Al 6061 #'s 101 and 102).


Figure B.13 Photos taken before and after cleaning of crevice (two of the same alloy mated together) coupons (Al 6061 #'s 103 and 104).


Figure B.14 Photos taken before and after cleaning of crevice (two of the same alloy mated together) coupons (Al 6063 #'s 137 and 138).


Figure B.15 Photos taken before and after cleaning of crevice (two of the same alloy mated together) coupons (Al 6063 #'s 139 and 140).

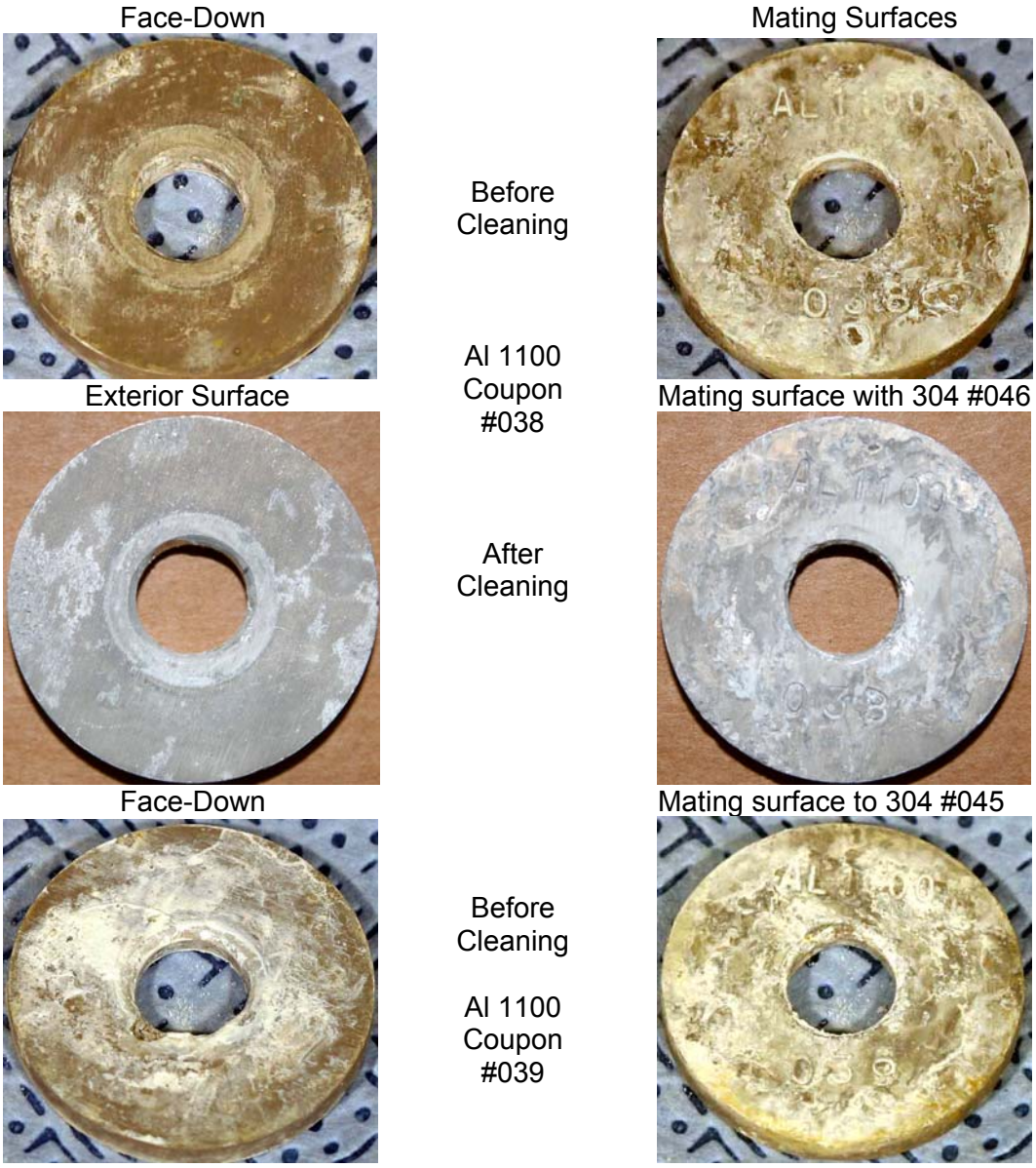


Figure B.16 Photos taken before and after cleaning of galvanic 1100 coupons, #'s 38 and 39 Coupon #39 was contaminated during surface analysis in the SEM and never cleaned.

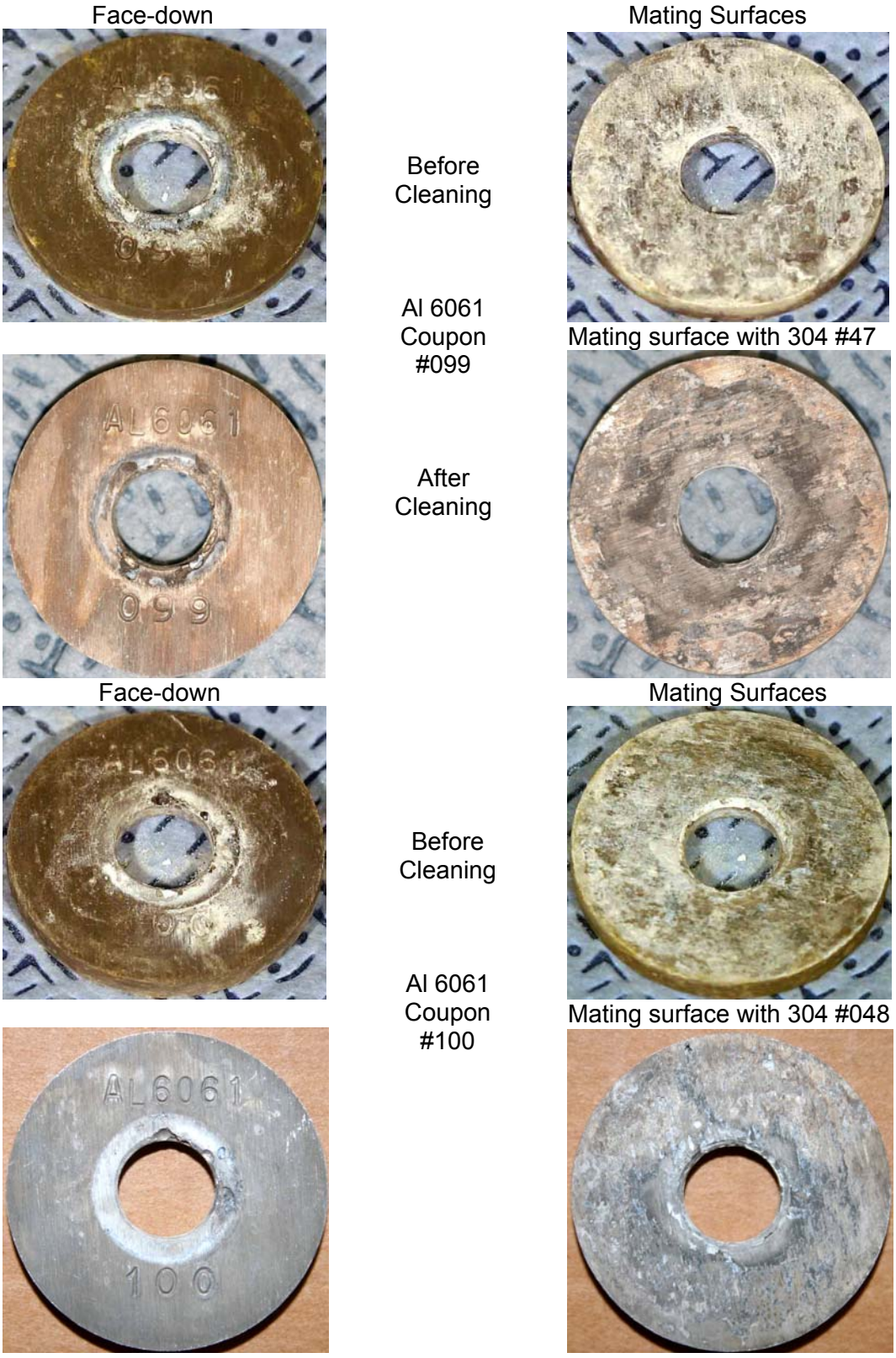


Figure B.17 Photos taken before and after cleaning of of galvanic 6061 coupons, #'s 99 and 100.


Figure B.18 Magnified surface of Al 6061 Coupon # 100 revealing deep pitting in crevice area below Teflon washer.

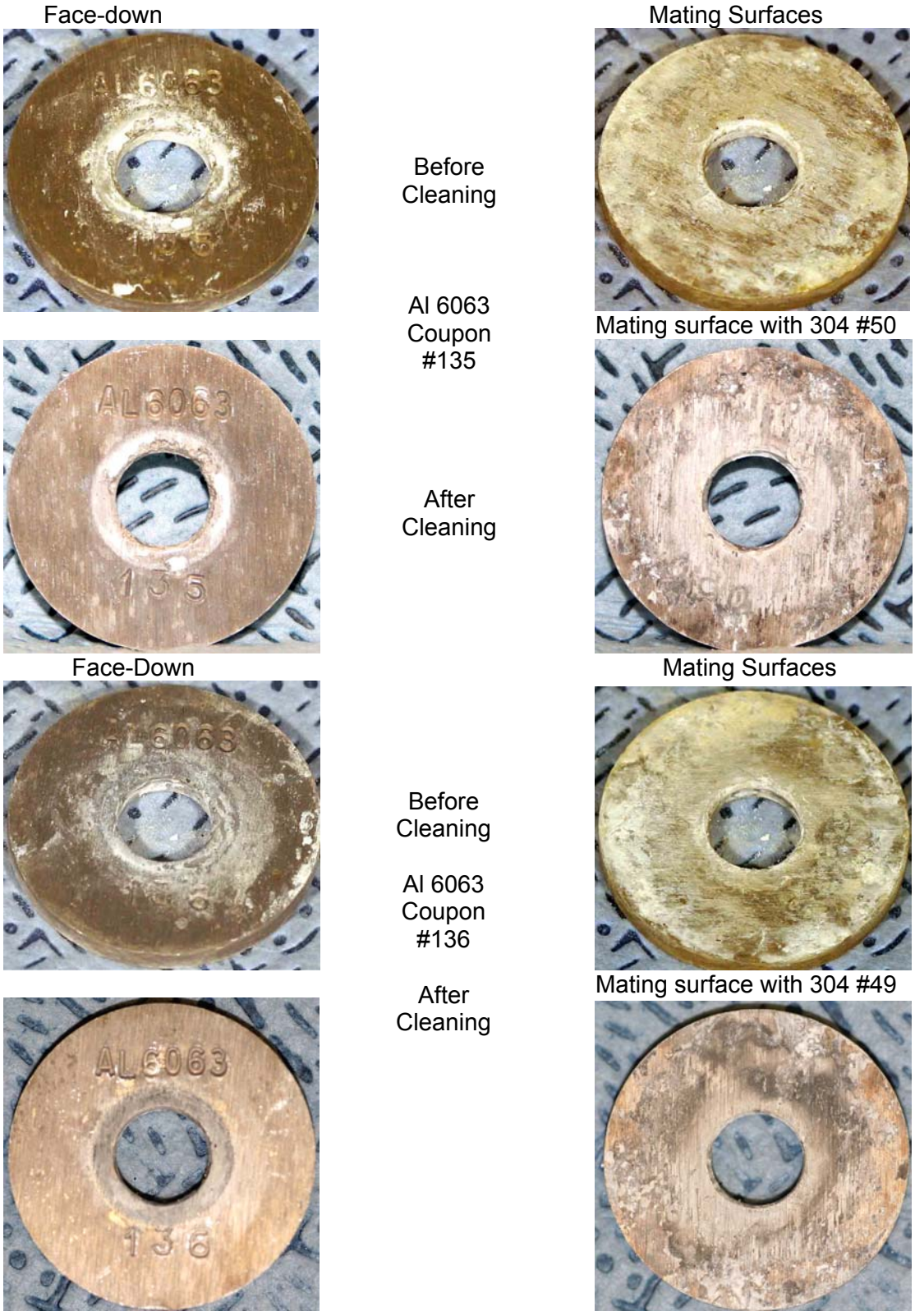


Figure B.19 Photos taken before and after cleaning of of galvanic 6063 coupons, #'s 135 and 136.

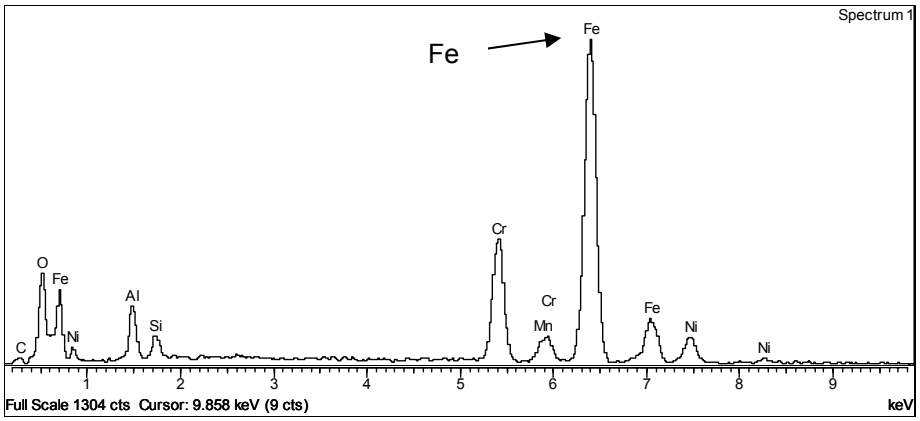


(A) EDS displays high Fe contents

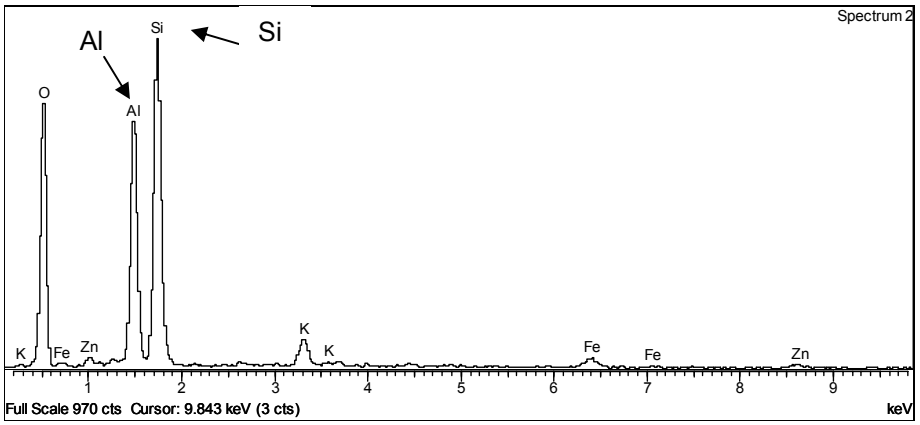


(B) EDS displays Si content higher than Al

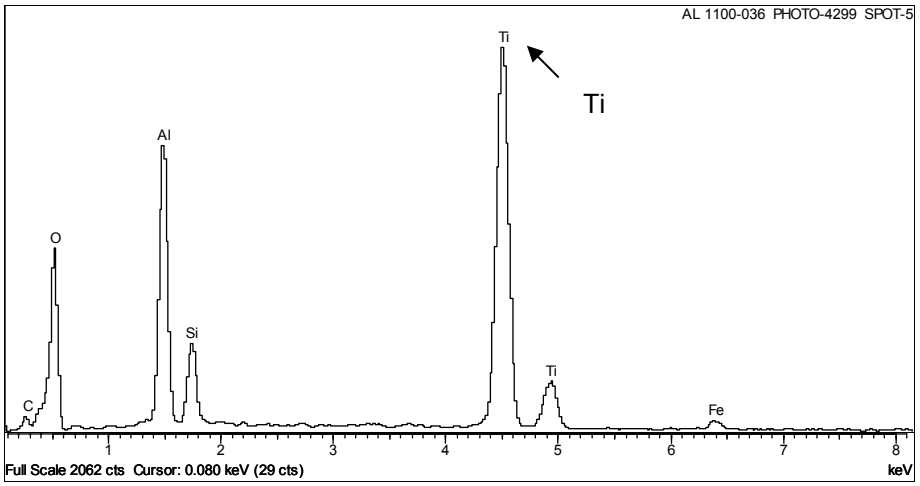


(C) EDS displays high Ti contents

Figure B.20 Spot analysis of an Al 1100 #036 coupon surface by energy dispersive spectroscopy (EDS) revealed areas containing Si, Ti, and Fe in addition to the expected Al and O.

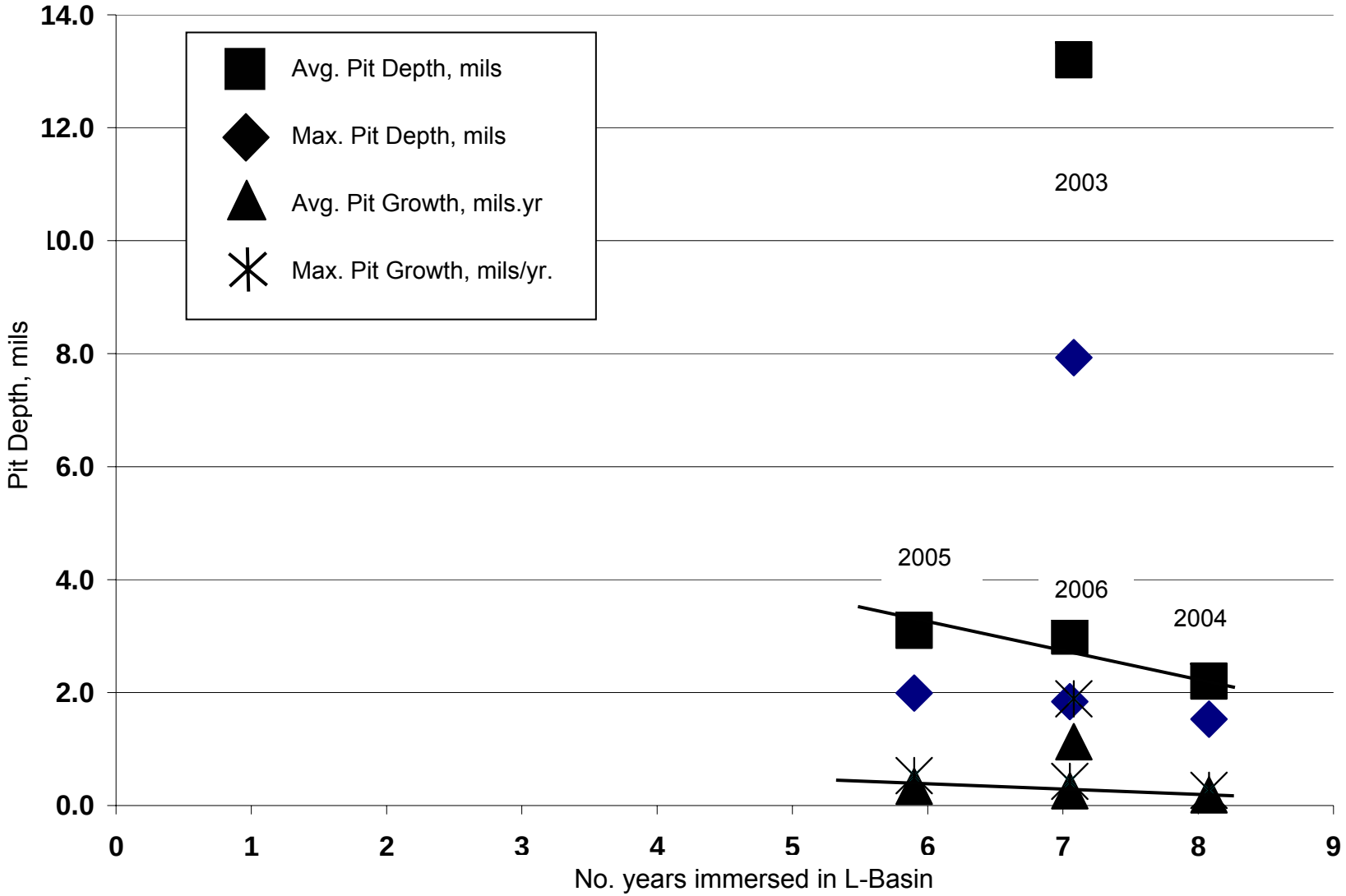


Figure B.21 Average and maximum pit data for Al1100 coupons removed in 2003, 2004, 2005, and 2006. The average and maximum 2003 data are beyond the drawn boundary lines compared to remaining data.

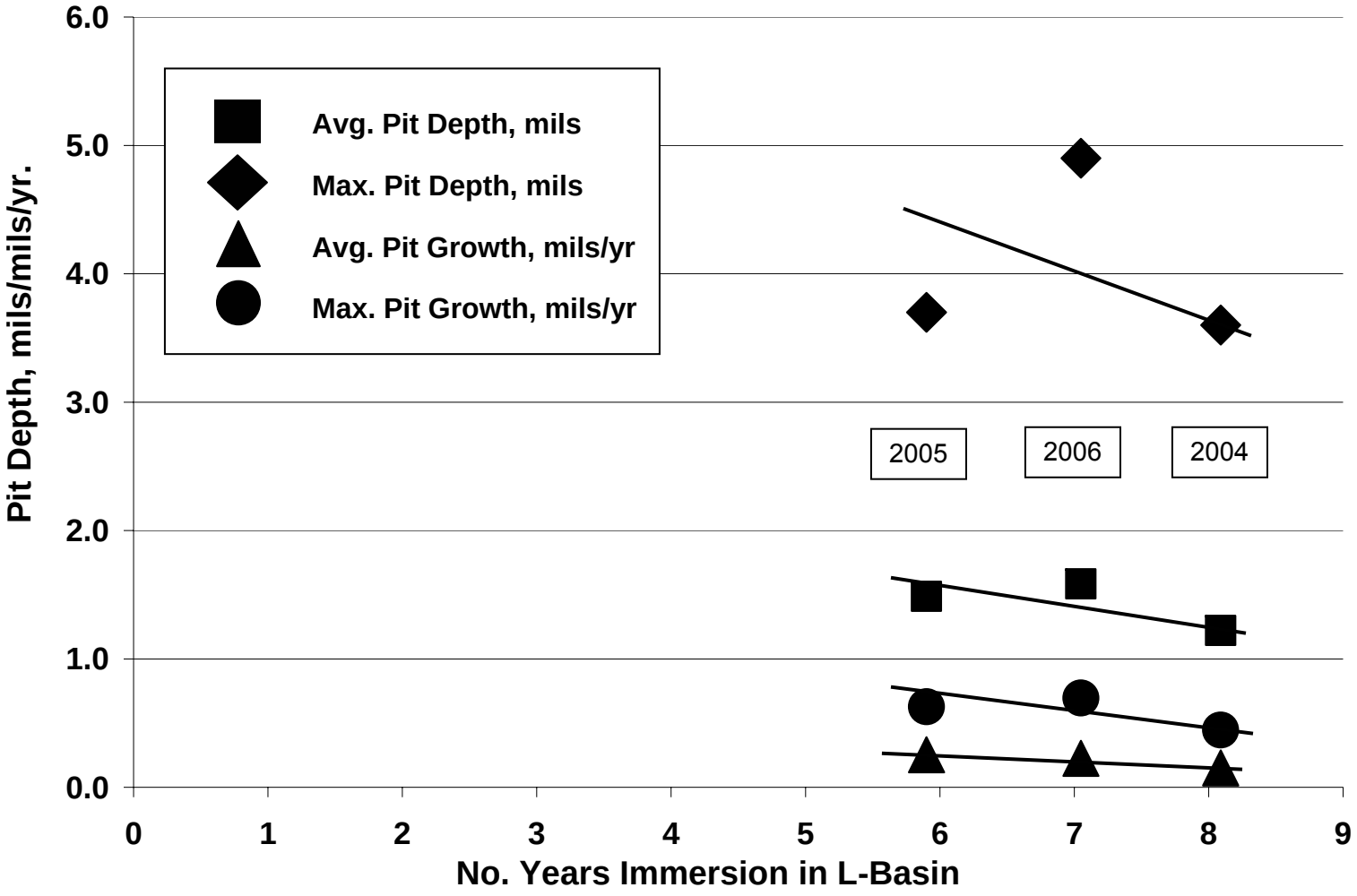


Figure B.22 Average and maximum pit data for Al 6061 coupons removed in 2004, 2005, and 2006.

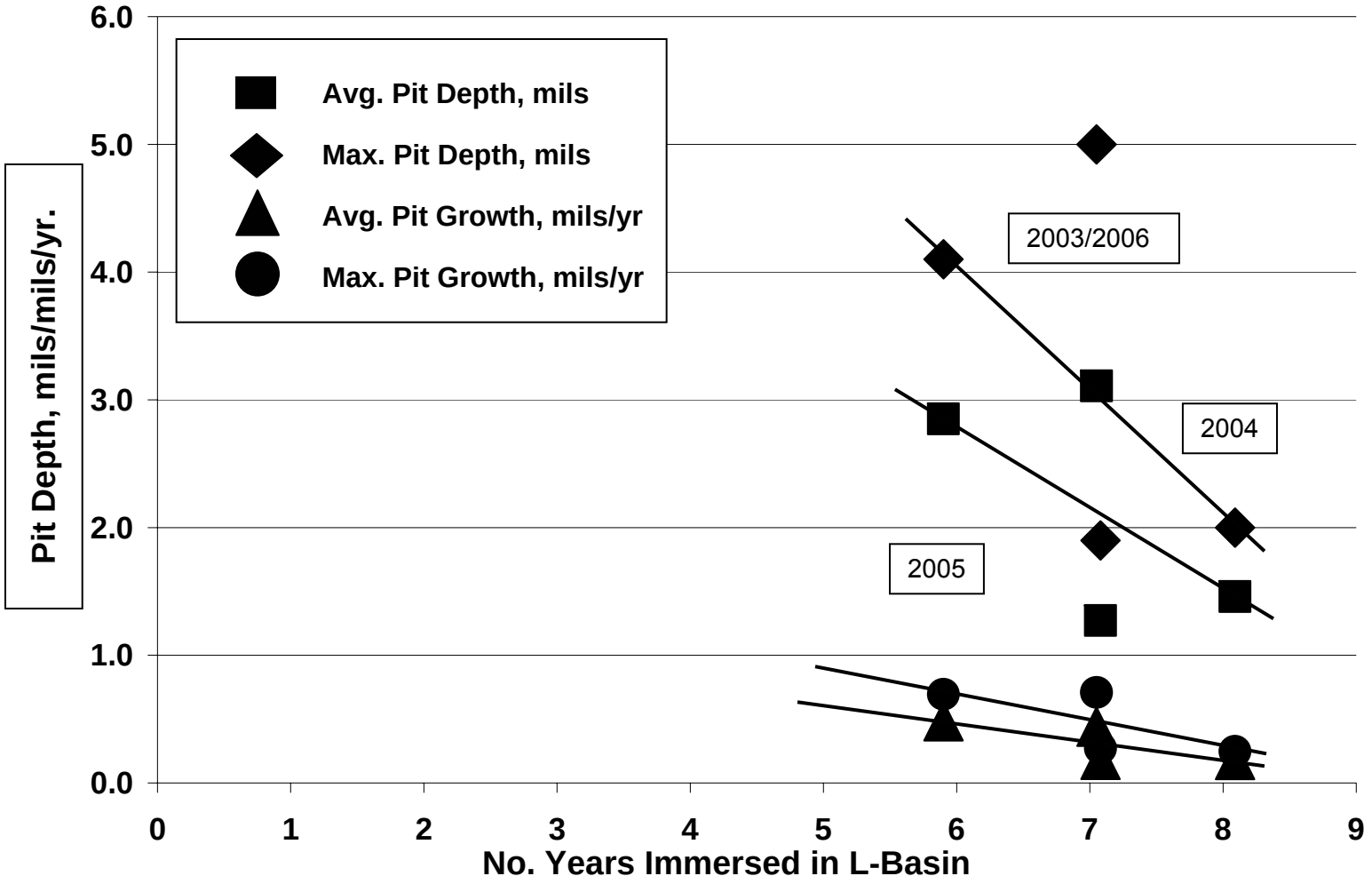


Figure B.23 Average and maximum pit data for Al 6063 coupons removed in 2003, 2004, 2005, and 2006.

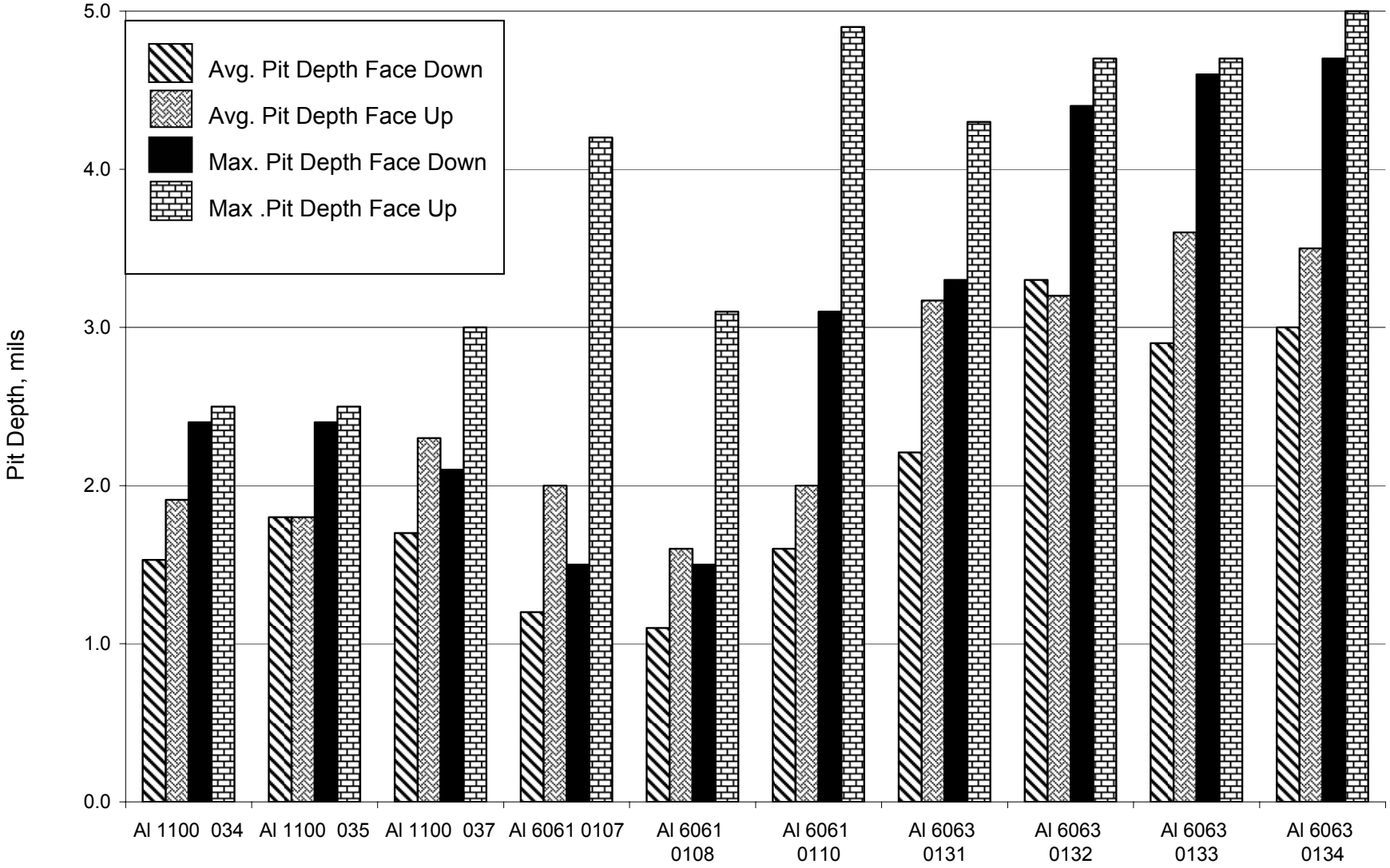


Figure B.24 Effect of aluminum alloy type and orientation on pit depths on 2006 corrosion surveillance coupons. These are individual coupons.

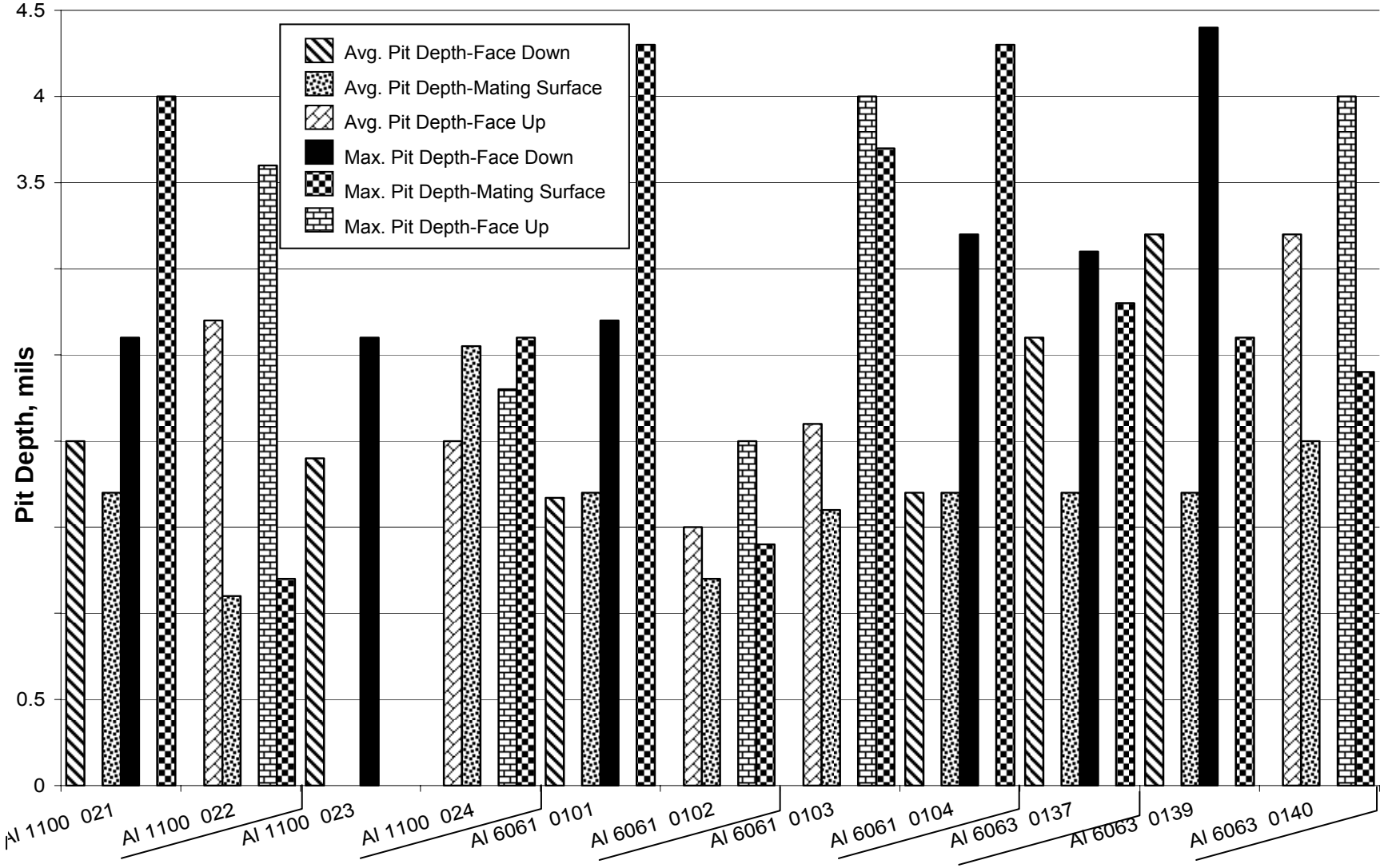


Figure B.25 Effect of crevice pairs, alloy type, and surface orientation on pit depths. The mating coupon to Al 5053 0137. was used for surface analysis.

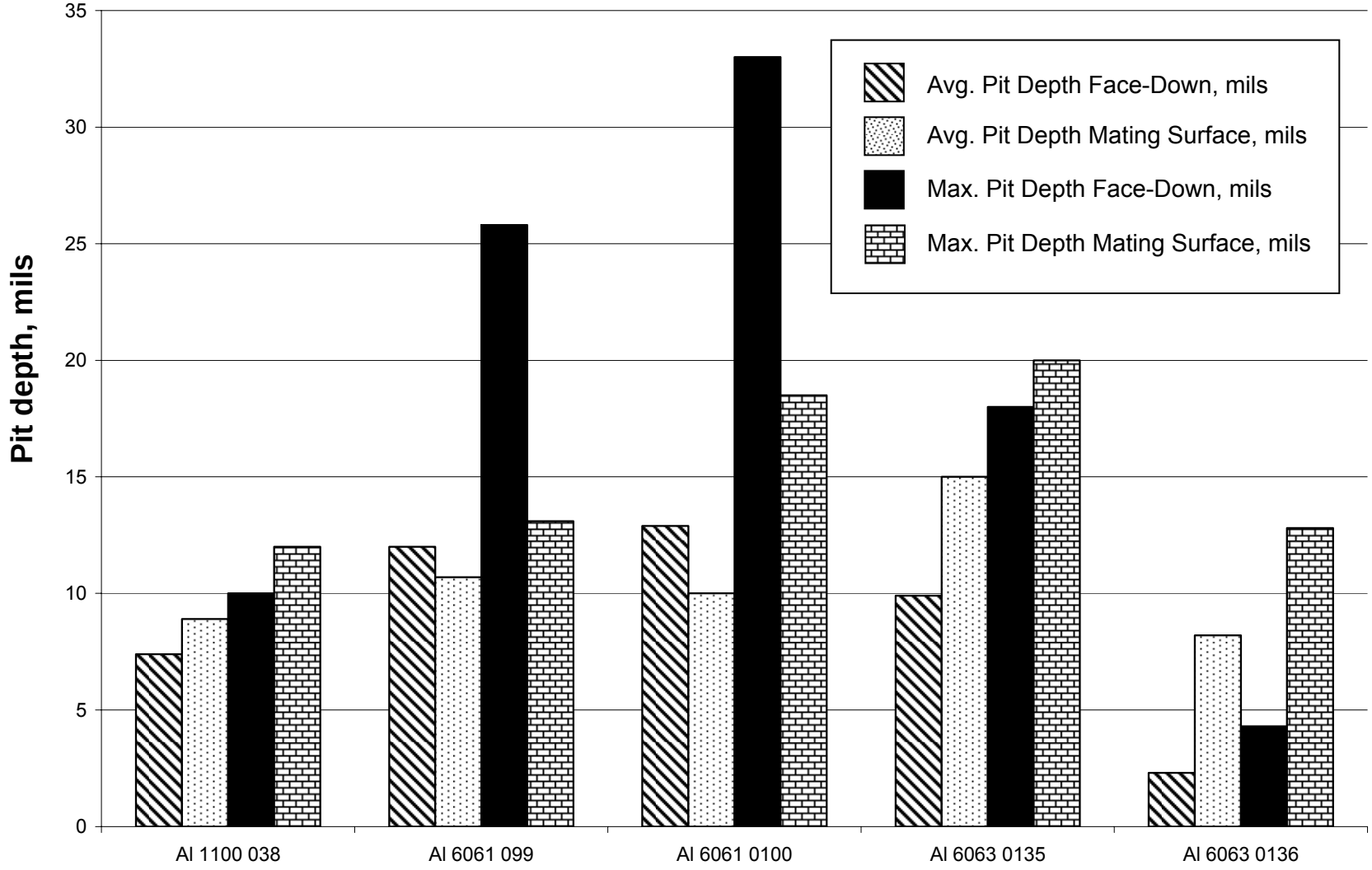


Figure B.26 Effect of galvanic coupon and orientation on pit depth.

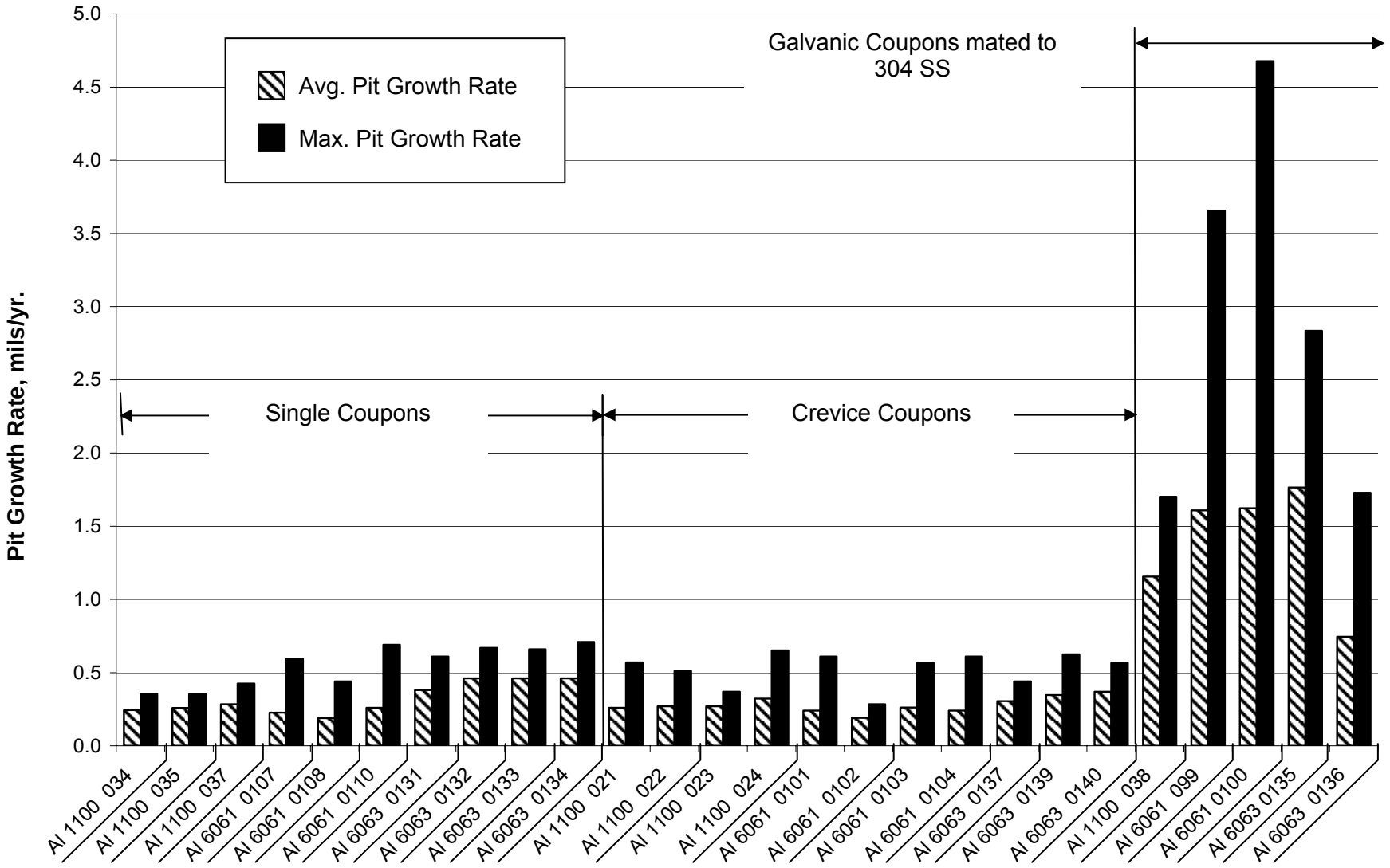


Figure B.27 Effect of coupon types and alloy on pit growth.

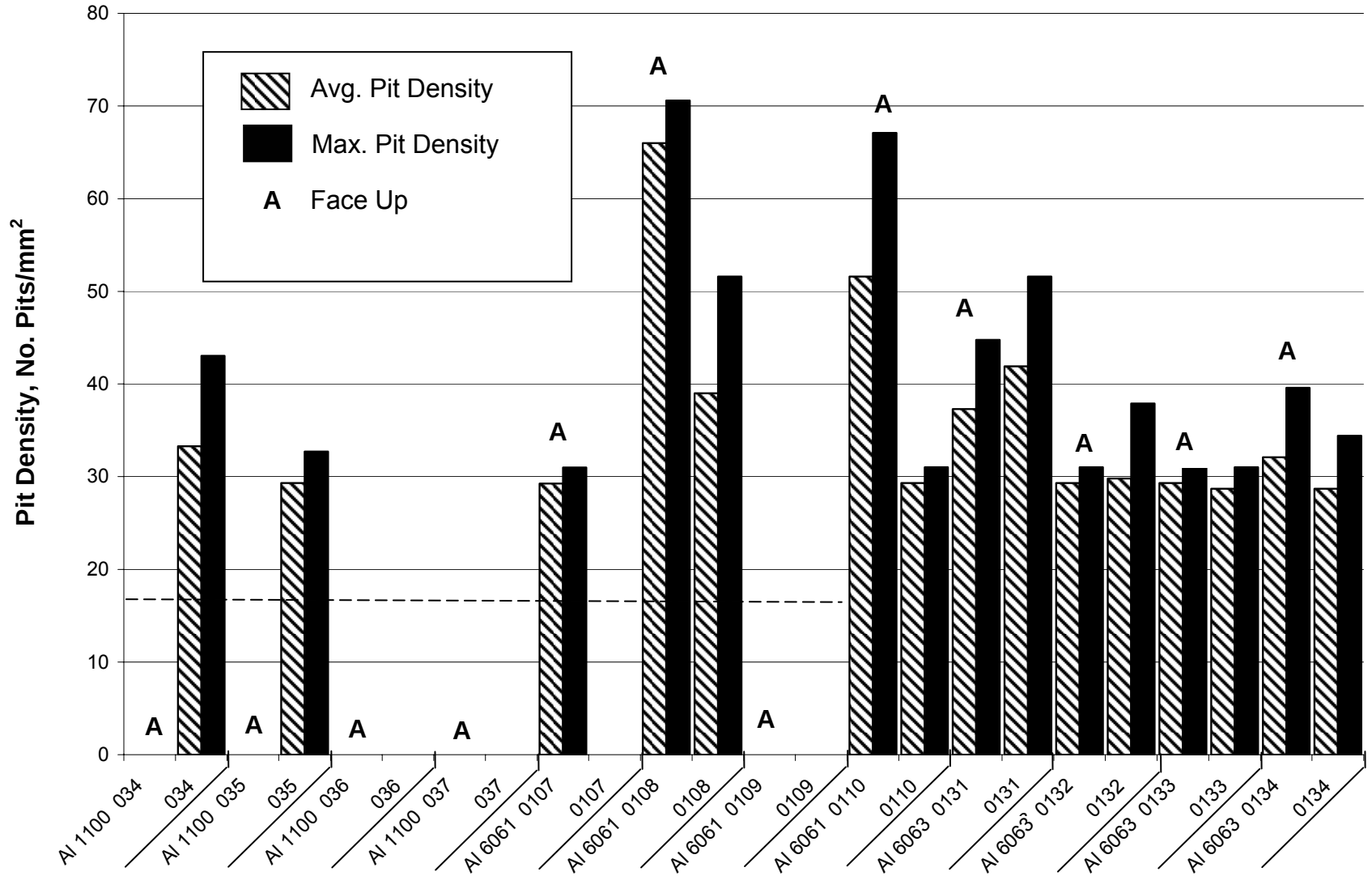


Figure B.28 Effect of single coupons, alloy type, and surface orientation on pit density. The dashed line indicates those surfaces without data displayed less than 10 pits in a single 0.5809 $mm^2$ area or less than a total of 50 pits in three separate 0.5809 $mm^2$ areas.

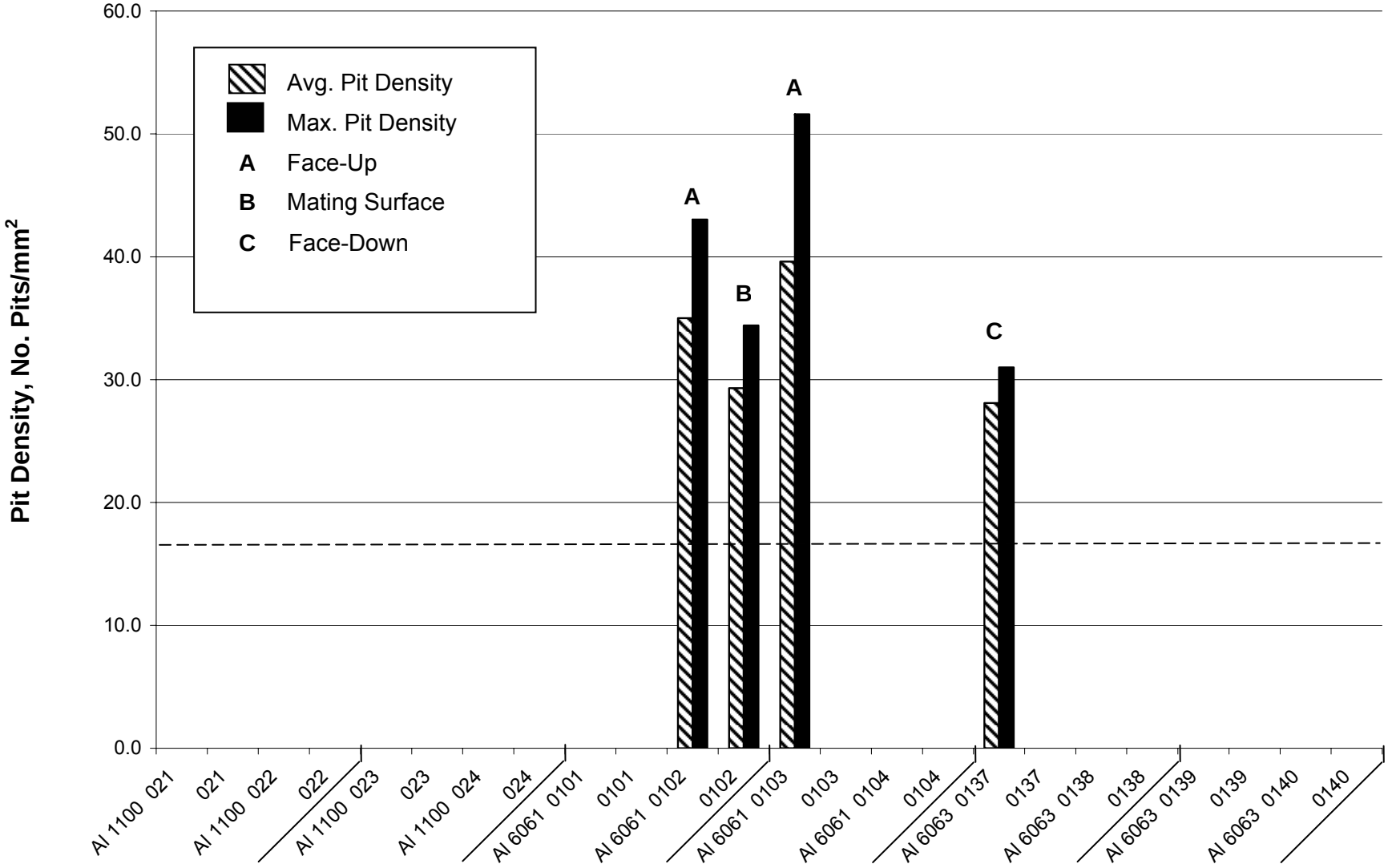


Figure B.29 Effect of crevice pairs, alloy type, and orientation on pit densities. The dashed line indicates those surfaces without data displayed less than 10 pits in a single 0.5809 $mm^2$ area or less than a total of 50 pits in three separate 0.5809 $mm^2$ areas.

## WSRC INTERNAL DISTRIBUTION

D. B. Rose, 704-28L
T. J. Spieker, 704-L
D. L. Melvin, 704-25L
R. W. Deible, 704-L
N. C. Iyer, 773-41A
R. L. Sindelar, 773-41A
D. W. Vinson, 773-41A
P. R. Vormelker, 773-41A
C. N. Foreman, 773-A
D. W. Vinson, 773-41A
W. C. Crouch, 773-41A